NASA TECHNICAL NOTE

NASA TN D-3539

NASA TN D-3539

SUPERSONIC AERODYNAMIC CHARACTERISTICS OF A SERIES OF RELATED BODIES WITH CROSS-SECTIONAL ELLIPTICITY

by Roger H. Fournier, Bernard Spencer, Jr. and William A. Corlett

Langley Research Center
Langley Station, Hampton, Va.

NATIONAL AERONAUTICS AND SPACE ADMINISTRATION • WASHINGTON, D. C. • AUGUST 1966

NASA TN D-3539

SUPERSONIC AERODYNAMIC CHARACTERISTICS OF A SERIES OF RELATED BODIES WITH CROSS-SECTIONAL ELLIPTICITY

By Roger H. Fournier, Bernard Spencer, Jr.,
and William A. Corlett

Langley Research Center
Langley Station, Hampton, Va.

NATIONAL AERONAUTICS AND SPACE ADMINISTRATION

For sale by the Clearinghouse for Federal Scientific and Technical Information
Springfield, Virginia 22151 – Price $3.00

SUPERSONIC AERODYNAMIC CHARACTERISTICS OF A SERIES OF RELATED BODIES WITH CROSS-SECTIONAL ELLIPTICITY

By Roger H. Fournier, Bernard Spencer, Jr.,
and William A. Corlett
Langley Research Center

SUMMARY

An investigation has been made in the Langley Unitary Plan wind tunnel to determine the supersonic aerodynamic characteristics of a series of power-law bodies and of a theoretical hypersonic minimum-wave-drag body of equal length and equal volume. Also included in the investigation are the effects of altering cross-sectional ellipticity for a given body while maintaining a constant longitudinal distribution of cross-sectional area. The Mach number range of the investigation was 1.50 to 4.63, and the angle of attack was varied from approximately -4° to 28° at 0° of sideslip.

Results indicate that increasing the power-body exponent for a given value of ellipticity results in increases in the lift-curve slope at low angles of attack. There are only slight effects of increasing the Mach number on the lift characteristics of the bodies tested. Except at a Mach number of 1.50, a minimum in the variation of minimum drag with increasing body exponent has been found at each Mach number. For all configurations, increasing the Mach number results in large reductions in minimum drag. At Mach numbers above 1.50, a maximum in the variation of the maximum lift-drag ratio with increasing body exponent has been found. This maximum occurs in the exponent region between 0.50 and 0.66, especially at the higher Mach numbers. For all configurations, increasing the Mach number results in large increases in the maximum lift-drag ratio. Increasing the power-body exponent results in large rearward shifts in the center-of-pressure location at all Mach numbers. Increasing the ellipticity for a given power-law body or for the minimum-wave-drag body results in large increases in lift and in the maximum lift-drag ratio with only slight effects on the center-of-pressure location at all Mach numbers. A comparison of the longitudinal aerodynamic characteristics of the theoretical hypersonic minimum-wave-drag body with the series of power-law bodies indicates that, for all values of ellipticity, the lift characteristics of this body generally fall in the range noted for the power-law bodies with exponents of 0.50 and 0.66. The minimum drag values for the minimum-wave-drag body are as low as or lower than those noted for any of the power-law bodies tested, and the maximum lift-drag ratios are generally as high as or higher than those noted for the power-law bodies.

INTRODUCTION

Extensive research related to the theoretical and experimental determination of the aerodynamic characteristics of volumetrically efficient lifting-body configurations has been done and is currently being done by the National Aeronautics and Space Administration and by others. (See, for example, refs. 1 to 9.) Configurations of this type may have application as vehicles designed for hypersonic cruise or glide or for operations between earth and near-earth orbiting laboratories. Since these missions will include a speed range from low-subsonic to hypersonic Mach numbers, aerodynamic efficiency in maneuvering ability and in range control is desired at all speeds (refs. 10 and 11).

In the continuing study of simplified lifting body shapes for hypersonic flight, the present investigation was undertaken to determine the supersonic aerodynamic characteristics of a series of power-law bodies and of a theoretical body of equal length and equal volume for minimizing zero-lift pressure drag at hypersonic speeds. The values of exponent for the power-law bodies were 0.25, 0.50, 0.66, 0.75, and 1.00. The hypersonic minimum-wave-drag shape was determined in accordance with the methods described in references 6 and 7. For a given power-law body and for the minimum-wave-drag body, the cross-sectional shape was altered from circular to elliptic while maintaining a constant longitudinal distribution of cross-sectional area. Horizontal- to vertical-axis ratios of 1.0, 2.0, and 3.0 were investigated for each of the power-law bodies and for the minimum-wave-drag body. The transonic aerodynamic characteristics of these models have been reported in reference 9.

The results presented herein were obtained in the Langley Unitary Plan wind tunnel at Mach numbers from 1.50 to 4.63, through a range of angles of attack from approximately -4° to 28° at 0° of sideslip, and at a constant Reynolds number of 5.73×10^6 (based on model length).

SYMBOLS

The forces and moments have been computed in coefficient form with respect to the projected planform area and length of each body. Data are referred to the stability-axis system with the longitudinal location of the moment reference selected as 66.67 percent of the total length, 25.00 inches (0.635 m), for each configuration. The vertical moment reference is located on the body center line.

a semimajor (horizontal) axis of elliptic-cross-section bodies, radius for $a/b = 1.0$ bodies, feet (meters)

a_{max} body maximum semispan, feet (meters)

A	aspect ratio, $\frac{(2a_{max})^2}{S}$
A_b	body base area, feet^2 (meters^2)
b	semiminor (vertical) axis of elliptic-cross-section bodies, feet (meters)
b_{max}	maximum vertical height at body base, feet (meters)
C_D	drag coefficient, $\frac{Drag}{qS}$
$C_{D,min}$	minimum drag coefficient
$C'_{D,min}$	minimum drag coefficient adjusted to a condition of free-stream pressure at model base
C_L	lift coefficient, $\frac{Lift}{qS}$
C_{L_α}	lift-curve slope measured between $\alpha \approx \pm 4^o$, through $\alpha = 0^o$, per degree
C_m	pitching-moment coefficient, $\frac{Pitching\ moment}{qSl}$
C_{m_α}	longitudinal stability parameter measured between $\alpha \approx \pm 4^o$, through $\alpha = 0^o$, per degree
C_{N_α}	normal-force-curve slope measured between $\alpha \approx \pm 4^o$, through $\alpha = 0^o$, per degree
C_p	pressure coefficient at base of model
l	total body length, inches (meters)
L/D	lift-drag ratio
$(L/D)_{max}$	maximum lift-drag ratio
$(L/D)'_{max}$	maximum lift-drag ratio adjusted to a condition of free-stream pressure at model base
M	free-stream Mach number

n	power-body exponent
q	free-stream dynamic pressure, pounds/foot^2 (newtons/meter^2)
S	body projected planform area (see fig. 3(b)), feet^2 (meters^2)
S_{cross}	cross-sectional area of bodies, feet^2 (meters^2)
S_{wet}	wetted area of bodies (excluding base area), feet^2 (meters^2)
x	longitudinal ordinate of bodies, feet (meters)
x_o	longitudinal ordinate of moment reference point, feet (meters)
x_{cp}/l	longitudinal center-of-pressure location ($\alpha \approx 0^o$), $\frac{x_o}{l} - \frac{C_{m_\alpha}}{C_{N_\alpha}}$
α	angle of attack, degrees

MODELS

The models used in this investigation consisted of 18 different body shapes and are 25.00 inches (0.635 m) in length. Details of the models are presented in figure 1. Photographs of the models are presented in figure 2. One group of bodies has circular cross sections with $a/b = 1.0$ (fig. 2(a)) and two groups have elliptic cross sections with $a/b = 2.0$ and $a/b = 3.0$ (figs. 2(b) and 2(c)). Body design ordinates are presented in table I. Pertinent geometric parameters associated with each of the models are presented in figure 3.

For each group, variations in semimajor and semiminor axis ordinates were derived from the following equations with geometric constraints imposed on the length and on the volume:

For horizontal projection (semimajor axis)

$$a = \frac{a_{max}}{l^n} x^n$$

and for vertical projection (semiminor axis)

$$b = \frac{b_{max}}{l^n} x^n$$

where values of n were 0.25, 0.50, 0.66, 0.75, and 1.00. The minimum-wave-drag bodies were determined in accordance with the methods of references 6 and 7, which theoretically minimized the zero-lift pressure drag at hypersonic speeds.

TESTS AND CORRECTIONS

The investigation was performed in both the low and the high Mach number test sections of the Langley Unitary Plan wind tunnel. The Mach numbers, stagnation pressures, and stagnation temperatures were as follows:

M	Stagnation pressure		Stagnation temperature	
	lb/ft^2, abs	kN/m^2	^oF	^oK
1.50	1530	73.26	150	338
1.90	1745	83.55	150	338
2.36	2165	103.66	150	338
2.86	2817	134.88	150	338
3.96	5294	253.48	175	352
4.63	7226	345.98	175	352

The stagnation dewpoint was maintained sufficiently low (-30^o F (238^o K)) to insure that no condensation effects would be encountered in the test sections. The tests were made through an angle-of-attack range from about -4^o to 28^o at a sideslip angle of 0^o and at a Reynolds number, based on body length, of 5.73×10^6. The angles of attack have been corrected for deflection of the balance and sting due to aerodynamic load. Static pressure measurements were taken at the model base and the data are presented as pressure coefficients in figure 4. The drag results presented herein include the effect of base pressure unless otherwise noted. Boundary-layer transition was artificially fixed with 1/16-inch-wide (0.16 cm) circumferential bands of carborundum grains having a nominal diameter of 0.012 inch (0.03 cm) affixed 1.0 inch (2.54 cm) behind the apex of each model.

RESULTS AND DISCUSSION

Comparisons of the basic longitudinal aerodynamic characteristics for the various configurations are presented in figures 5 to 10 as functions of angle of attack for Mach numbers from 1.50 to 4.63. These results are summarized in figures 11 to 14 in the form of the longitudinal parameters C_{L_α}, $C_{D,min}$, $C'_{D,min}$, $(L/D)_{max}$, $(L/D)'_{max}$, and x_{cp}/l plotted as functions of body exponent and Mach number.

Increasing the body exponent n (decreasing bluntness and increasing span) for a given value of ellipticity results in increases in the lift-curve slope at low angles of attack

at all Mach numbers (fig. 11(a)). The variation in lift coefficient with angle of attack for the minimum-wave-drag body generally falls between that of the $n = 0.50$ and $n = 0.66$ bodies for any ellipticity and for all Mach numbers. (See part (a) of figs. 5 to 10.)

Increasing the ellipticity for all configurations results in large increases in the lift-curve slope at low angles of attack at all Mach numbers (figs. 11(a) and 11(b)). This increase in C_{L_α} is primarily due to the increasing aspect ratio associated with increasing ellipticity. There are only slight effects of increasing the Mach number on the lift-curve-slope characteristics for the configurations tested (fig. 11(b)).

Increasing the value of body exponent n from 0.25 to 1.00 for a given value of ellipticity results in large continuous increases in $C_{D,min}$ at a Mach number of 1.50 (fig. 12(a)). At Mach numbers above 1.50, however, there is an increase in the value of body exponent n at which a minimum in the $C_{D,min}$ variation with n occurs (fig. 12(a)). The minimum drag level of the minimum-wave-drag body is essentially the same as the lowest $C_{D,min}$ value noted for the power-law bodies for corresponding ellipticities (fig. 12(a)). In figure 12(b), the large reductions in $C_{D,min}$ which occur for each configuration tested as the Mach number is increased from 1.50 to 4.63 are primarily due to the large decrease in base drag with increasing Mach number (indicated by the C_p variations presented in fig. 4).

Examination of the $C'_{D,min}$ curves of figure 12(c) shows that the minimum values of $C'_{D,min}$ are in the range of n values between about 0.50 and 0.60 for all Mach numbers. Examination of the drag data results of (fig. 12(d)) shows only a small variation in $C'_{D,min}$ with Mach number. Again, this indicates the sizable effects of base drag on configurations of this type.

The effects of body exponent and Mach number on $(L/D)_{max}$ are presented for configurations of varying ellipticity in figures 13(a) and 13(b). Increasing the body exponent n for a given value of ellipticity indicates only slight effects on $(L/D)_{max}$ at the lower test Mach number (fig. 13(a) at $M = 1.50$). However, as the Mach number approaches 4.63, a maximum in the variation of $(L/D)_{max}$ with n occurs in the region between $n = 0.50$ and $n = 0.66$ (fig. 13(a)). Large increases in $(L/D)_{max}$ occur with increasing ellipticity for all configurations tested at all Mach numbers. The $(L/D)_{max}$ values noted for the minimum-wave-drag body are as high as or higher than those noted for any of the series of power-law bodies tested for corresponding values of ellipticity at all Mach numbers (fig. 13(a)). Increasing the Mach number (fig. 13(b)) generally results in increases in $(L/D)_{max}$ for the various bodies for all values of ellipticity, primarily due to the large reduction in base axial force with increasing Mach numbers, as previously noted.

The $(L/D)'_{max}$ characteristics for the various configurations are presented in figures 13(c) and 13(d) as functions of power-body exponent and of Mach number,

respectively. The data generally indicate that the highest value of $(L/D)'_{max}$ occurs in the region between $n = 0.50$ and $n = 0.75$ for all values of ellipticity and at all Mach numbers (fig. 13(c)). The $(L/D)'_{max}$ characteristics of the minimum-wave-drag body indicate that, at the higher Mach numbers ($M = 3.96$ and 4.63), the values of $(L/D)'_{max}$ for these bodies are generally as high as or higher than those for any of the power-law bodies tested. However, at the lower Mach numbers, the power-law bodies generally have slightly higher values of $(L/D)'_{max}$.

The effects of body exponent and Mach number on center-of-pressure location (x_{cp}/l) are shown in figures 14(a) and 14(b), respectively. A large rearward shift of x_{cp}/l with increasing body exponent is noted at all Mach numbers for all values of ellipticity (fig. 14(a)). The values of x_{cp}/l for the theoretical minimum-wave-drag body fall between those noted for the $n = 0.50$ and $n = 0.66$ bodies. There are only minor effects of increasing the ellipticity for a given power-law body or for the minimum-wave-drag body (except for $n = 0.25$) at all Mach numbers (fig. 14(b)). There are little or no effects of increasing the Mach number on the x_{cp}/l characteristics for any configuration investigated, except for the $n = 0.25$ power-law body.

CONCLUSIONS

An investigation has been made in the Langley Unitary Plan wind tunnel to determine the supersonic aerodynamic characteristics of a series of power-law bodies and of a theoretical hypersonic minimum-wave-drag body of equal length and equal volume. Also included in the investigation are the effects of altering cross-sectional ellipticity for a given body while maintaining a constant longitudinal distribution of cross-sectional area. The Mach number range of the investigation was 1.50 to 4.63, and the angle of attack was varied from approximately -4^o to 28^o at 0^o of sideslip. The results of this investigation can be summarized in the following observations:

1. Increasing the power-body exponent for a given value of ellipticity results in increases in the lift-curve slope at low angles of attack. There are only slight effects of increasing the Mach number on the lift characteristics of the bodies tested. Except at a Mach number of 1.50, a minimum in the variation of minimum drag with increasing body exponent has been found at each Mach number. For all configurations, increasing the Mach number results in large reductions in minimum drag. At Mach numbers above 1.50, a maximum in the variation of maximum lift-drag ratio with increasing body exponent has been found. This maximum occurs in the exponent region between 0.50 and 0.66, especially at the higher Mach numbers. For all configurations, increasing the Mach number results in large increases in the maximum lift-drag ratio. Increasing the power-body exponent results in large rearward shifts in the center-of-pressure location at all Mach numbers.

2. Increasing the ellipticity for a given power-law body or for the minimum-wave-drag body results in large increases in lift and maximum lift-drag ratio with only slight effects on the center-of-pressure location at all Mach numbers, except for the lowest power-law body.

3. A comparison of the longitudinal aerodynamic characteristics of the theoretical hypersonic minimum-wave-drag body with the series of power-law bodies indicates that, for all values of ellipticity, the lift characteristics of this body generally fall in the range noted for the power-law bodies with exponents of 0.50 and 0.66. The minimum drag values for the minimum-wave-drag body are as low as or lower than those noted for any of the power-law bodies tested and the maximum lift-drag ratios are generally as high as or higher than those noted for the power-law bodies, particularly at the higher test Mach numbers.

Langley Research Center,
National Aeronautics and Space Administration,
Langley Station, Hampton, Va., April 12, 1966.

REFERENCES

1. Jorgensen, Leland H.: Elliptic Cones Alone and With Wings at Supersonic Speeds. NACA Rept. 1376, 1958. (Supersedes NACA TN 4045.)

2. Spencer, Bernard, Jr.; and Phillips, W. Pelham: Effects of Cross-Section Shape on the Low-Speed Aerodynamic Characteristics of a Low-Wave-Drag Hypersonic Body. NASA TN D-1963, 1963.

3. Fuller, Dennis E.; Shaw, David S.; and Wassum, Donald L.: Effect of Cross-Section Shape on the Aerodynamic Characteristics of Bodies at Mach Numbers From 2.50 to 4.63. NASA TN D-1620, 1963.

4. Spencer, Bernard, Jr.; Phillips, W. Pelham; and Fournier, Roger H.: Supersonic Aerodynamic Characteristics of a Series of Bodies Having Variations in Fineness Ratio and Cross-Section Ellipticity. NASA TN D-2389, 1964.

5. Spencer, Bernard, Jr.; and Phillips, W. Pelham: Transonic Aerodynamic Characteristics of a Series of Bodies Having Variations in Fineness Ratio and Cross-Sectional Ellipticity. NASA TN D-2622, 1965.

6. Eggers, A. J., Jr.; Resnikoff, Meyer M.; and Dennis, David H.: Bodies of Revolution Having Minimum Drag at High Supersonic Airspeeds. NACA Rept. 1306, 1957. (Supersedes NACA TN 3666.)

7. Suddath, Jerrold H.; and Oehman, Waldo I.: Minimum Drag Bodies With Cross-Sectional Ellipticity. NASA TN D-2432, 1964.

8. Miele, Angelo; Pritchard, Robert E.; and Hull, David G.: General Theory of Optimum Hypersonic Slender Bodies Including Frictional Effects. J. Astronaut. Sci., vol. X, no. 2, 1963, pp. 41-54.

9. Spencer, Bernard, Jr.: Transonic Aerodynamic Characteristics of a Series of Related Bodies With Cross-Sectional Ellipticity. NASA TN D-3203, 1966.

10. Baradell, Donald L.; and McLellan, Charles H.: Lateral-Range and Hypersonic Lift-Drag-Ratio Requirements for Efficient Ferry Service From a Near-Earth Manned Space Station. 2nd Manned Space Flight Meeting (Dallas, Texas), Am. Inst. Aeron. Astronaut., Apr. 1963, pp. 159-166.

11. Gregory, Thomas J.; Petersen, Richard H.; and Wyss, John A.: Performance Trade-Offs and Research Problems for Hypersonic Transports. Paper No. 64-605, Am. Inst. Aeron. Astronaut., Aug. 1964.

TABLE I.- DESIGN BODY ORDINATES

x/l	a/b = 1.0	a/b = 2.0		a/b = 3.0	
	a/l	a/l	b/l	a/l	b/l
		n = 0.25			
0	0	0	0	0	0
.0080	.0212	.0299	.0150	.0366	.0122
.0100	.0224	.0316	.0158	.0387	.0129
.0200	.0266	.0376	.0188	.0460	.0154
.0300	.0295	.0417	.0209	.0511	.0170
.0400	.0316	.0447	.0222	.0548	.0183
.0600	.0350	.0496	.0248	.0607	.0202
.1000	.0398	.0563	.0281	.0689	.0230
.1200	.0417	.0589	.0306	.0722	.0241
.2000	.0473	.0669	.0335	.0820	.0273
.2800	.0515	.0728	.0364	.0892	.0297
.3600	.0548	.0776	.0388	.0950	.0317
.5200	.0601	.0850	.0425	.1041	.0347
.6800	.0643	.0909	.0454	.1113	.0371
.8400	.0678	.0958	.0479	.1174	.0391
1.0000	.0708	.1001	.0500	.1226	.0408
		n = 0.50			
0	0	0	0	0	0
.0050	.0058	.0081	.0041	.0100	.0033
.0100	.0082	.0115	.0058	.0141	.0047
.0200	.0116	.0163	.0082	.0200	.0067
.0400	.0163	.0231	.0115	.0283	.0094
.0600	.0200	.0283	.0141	.0346	.0115
.1200	.0283	.0400	.0200	.0490	.0164
.2000	.0366	.0517	.0259	.0633	.0211
.2800	.0432	.0612	.0306	.0749	.0250
.3600	.0490	.0694	.0347	.0849	.0283
.4400	.0542	.0766	.0383	.0939	.0313
.5200	.0590	.0834	.0417	.1021	.0340
.6000	.0633	.0895	.0448	.1097	.0366
.6800	.0674	.0953	.0477	.1167	.0389
.7600	.0713	.1008	.0504	.1235	.0412
.8400	.0749	.1060	.0530	.1298	.0433
.9200	.0784	.1109	.0554	.1358	.0453
1.0000	.0818	.1156	.0578	.1416	.0472
		n = 0.66			
0	0	0	0	0	0
.0400	.0103	.0146	.0073	.0179	.0060
.1200	.0215	.0304	.0152	.0372	.0124
.2000	.0302	.0427	.0214	.0523	.0174
.2800	.0378	.0534	.0267	.0655	.0218
.3600	.0447	.0632	.0316	.0774	.0258
.4400	.0511	.0722	.0361	.0885	.0295
.5200	.0571	.0807	.0404	.0989	.0330
.6000	.0628	.0888	.0444	.1088	.0362
.6800	.0682	.0965	.0482	.1182	.0394
.7600	.0735	.1040	.0520	.1273	.0424
.8400	.0786	.1111	.0556	.1273	.0454
.9200	.0835	.1181	.0590	.1447	.0482
1.0000	.0883	.1248	.0624	.1529	.0510

TABLE I.- DESIGN BODY ORDINATES – Concluded

x/l	a/b = 1.0	a/b = 2.0		a/b = 3.0	
	a/l	a/l	b/l	a/l	b/l
		n = 0.75			
0	0	0	0	0	0
.0400	.0082	.0115	.0058	.0141	.0047
.1200	.0186	.0264	.0132	.0323	.0108
.2000	.0273	.0386	.0193	.0473	.0158
.2800	.0352	.0497	.0249	.0609	.0203
.3600	.0425	.0601	.0300	.0736	.0245
.4400	.0494	.0698	.0349	.0855	.0285
.5200	.0560	.0791	.0396	.0969	.0323
.6000	.0623	.0881	.0441	.1079	.0360
.6800	.0684	.0968	.0484	.1185	.0395
.7600	.0744	.1052	.0526	.1289	.0430
.8400	.0802	.1134	.0567	.1389	.0463
.9200	.0858	.1214	.0607	.1487	.0496
1.0000	.0914	.1292	.0646	.1583	.0528
		n = 1.00			
0	0	0	0	0	0
.0400	.0040	.0057	.0028	.0069	.0023
.1200	.0120	.0170	.0085	.0208	.0069
.2000	.0200	.0283	.0141	.0346	.0115
.2800	.0280	.0396	.0198	.0485	.0162
.3600	.0360	.0513	.0254	.0624	.0208
.4400	.0440	.0622	.0311	.0762	.0254
.5200	.0520	.0735	.0368	.0901	.0300
.6000	.0600	.0848	.0424	.1039	.0346
.6800	.0680	.0962	.0481	.1178	.0393
.7600	.0760	.1075	.0537	.1316	.0439
.8400	.0840	.1188	.0594	.1455	.0485
.9200	.0920	.1301	.0650	.1593	.0531
1.0000	.1000	.1414	.0707	.1732	.0577
		Minimum-wave-drag body			
0	0	0	0	0	0
.0400	.0098	.0139	.0070	.0170	.0057
.0800	.0161	.0228	.0114	.0279	.0093
.1200	.0216	.0305	.0153	.0373	.0124
.2000	.0312	.0441	.0221	.0540	.0180
.2800	.0396	.0560	.0280	.0686	.0229
.3600	.0469	.0663	.0332	.0813	.0271
.4400	.0534	.0775	.0388	.0924	.0308
.5200	.0592	.0837	.0419	.1025	.0342
.6000	.0646	.0913	.0457	.1119	.0373
.6800	.0695	.0982	.0491	.1203	.0401
.7600	.0738	.1043	.0521	.1278	.0426
.8400	.0773	.1093	.0542	.1338	.0446
.9200	.0800	.1131	.0565	.1385	.0462
1.0000	.0814	.1151	.0575	.1410	.0470

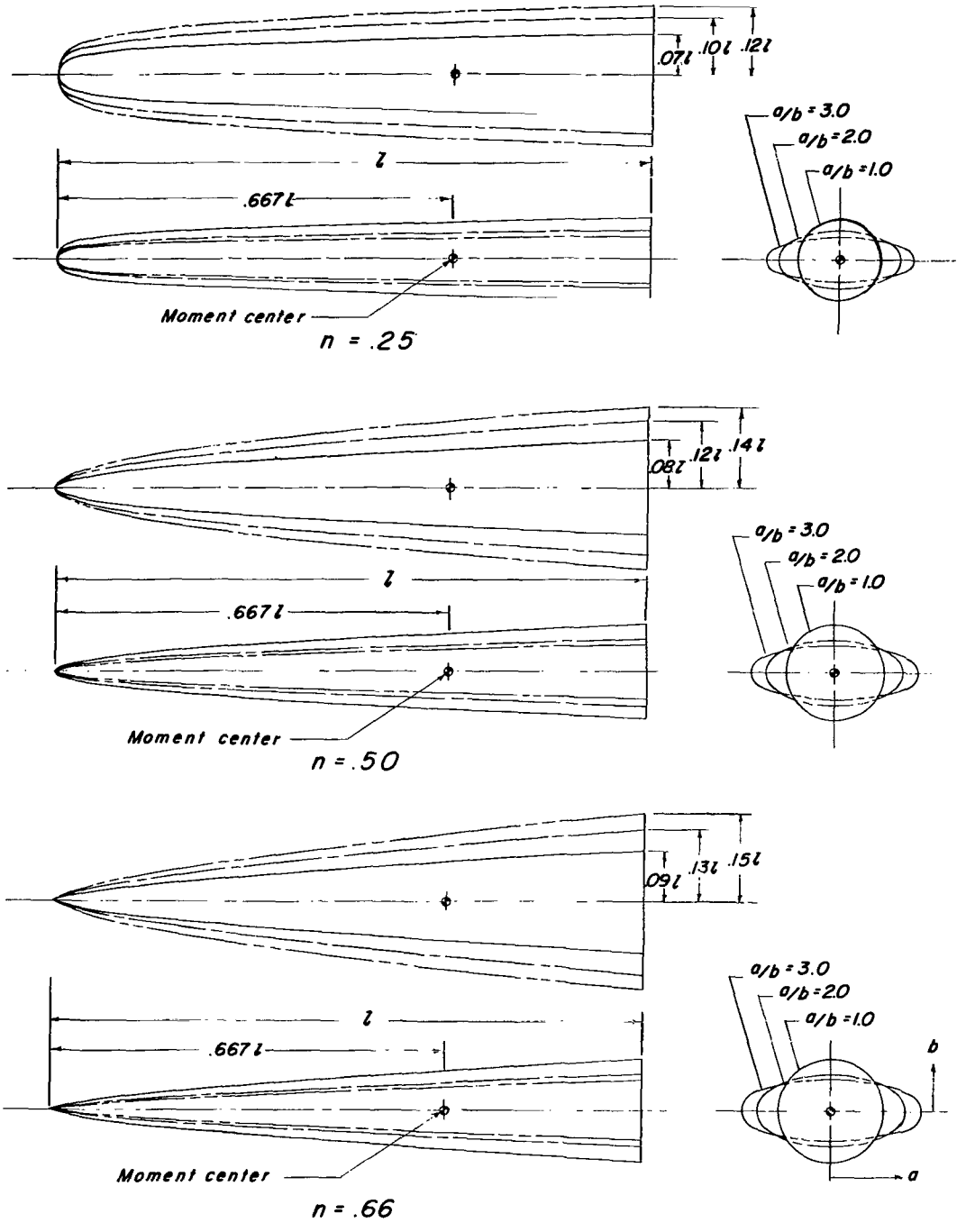

(a) n = 0.25, 0.50, and 0.66.

Figure 1.- Drawings of the various models tested.

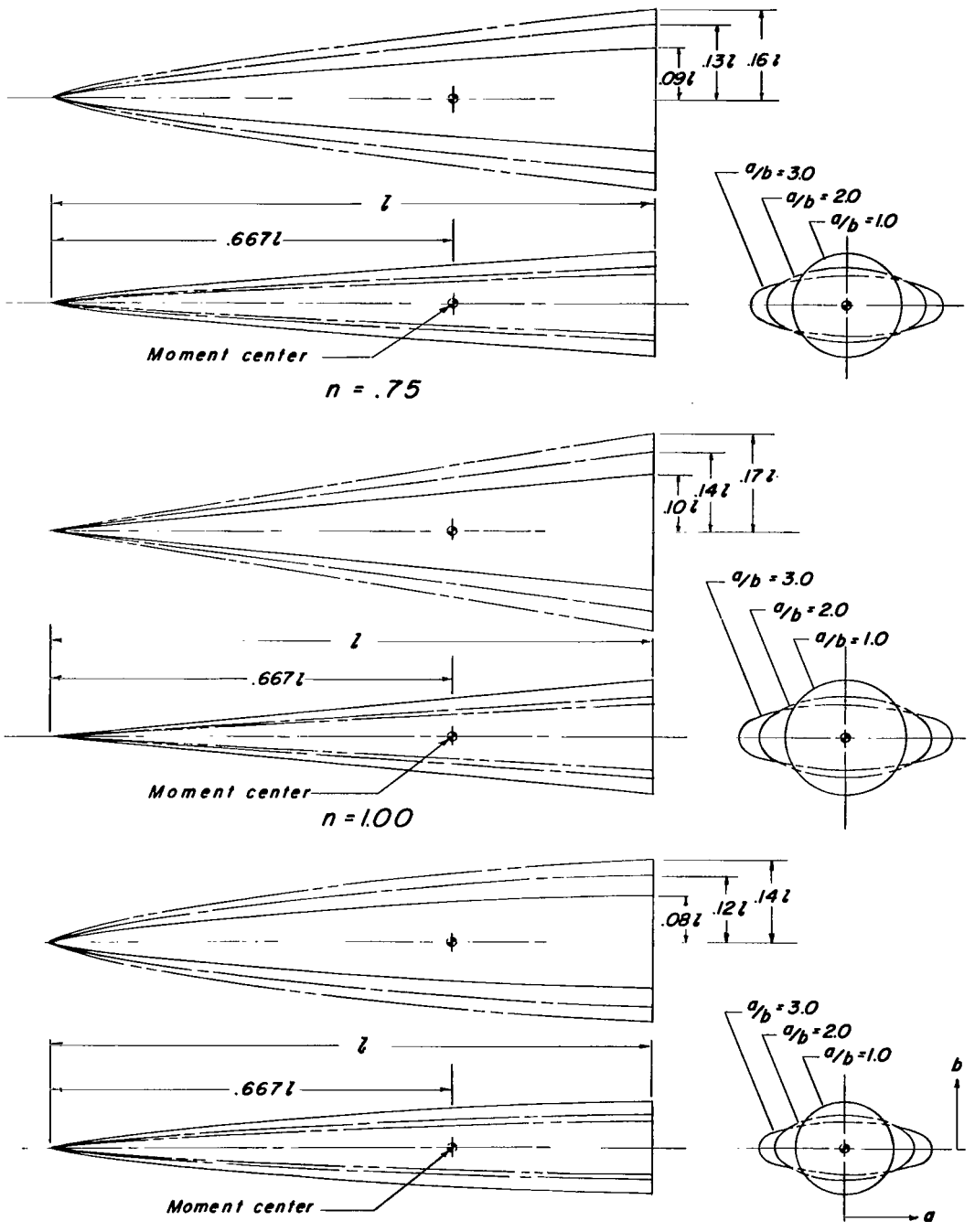

(b) n = 0.75, 1.00 and minimum-wave-drag body.

Figure 1.- Concluded.

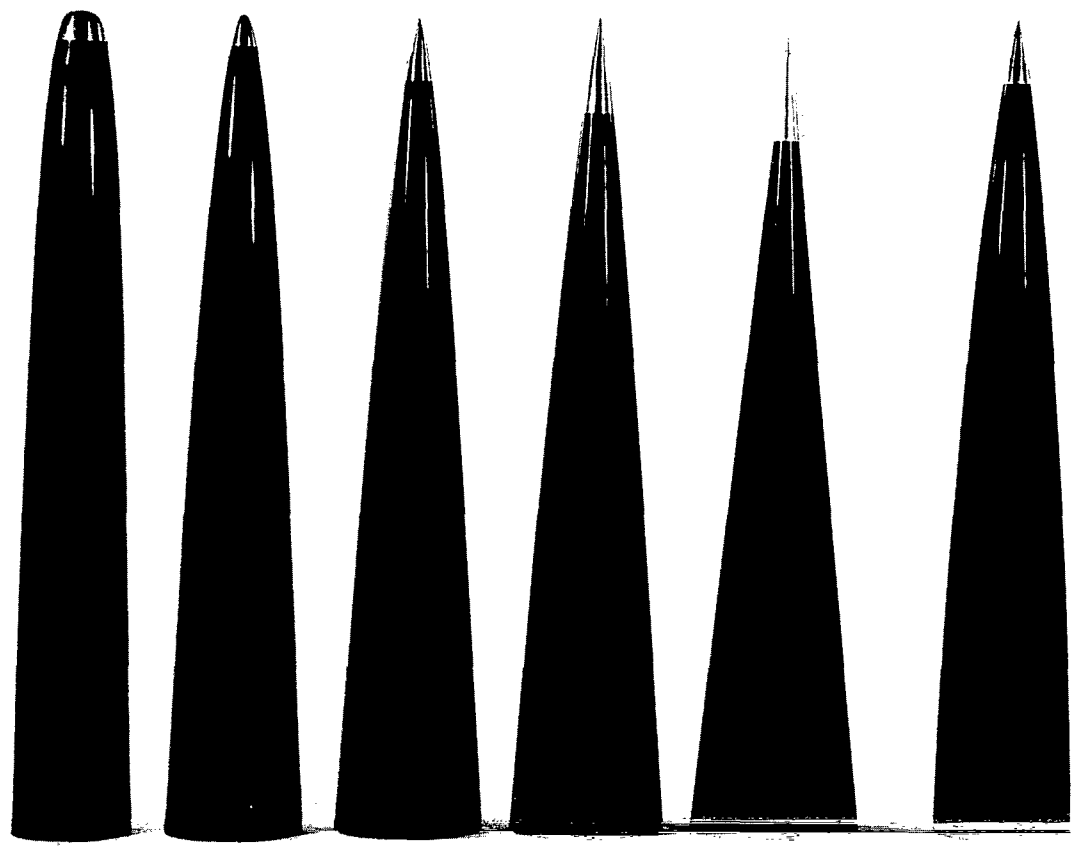

n = 0.25 n = 0.50 n = 0.66 n = 0.75 n = 1.00 Min. drag

(a) a/b = 1.0.

L-65-2660

Figure 2.- Photographs of the models tested.

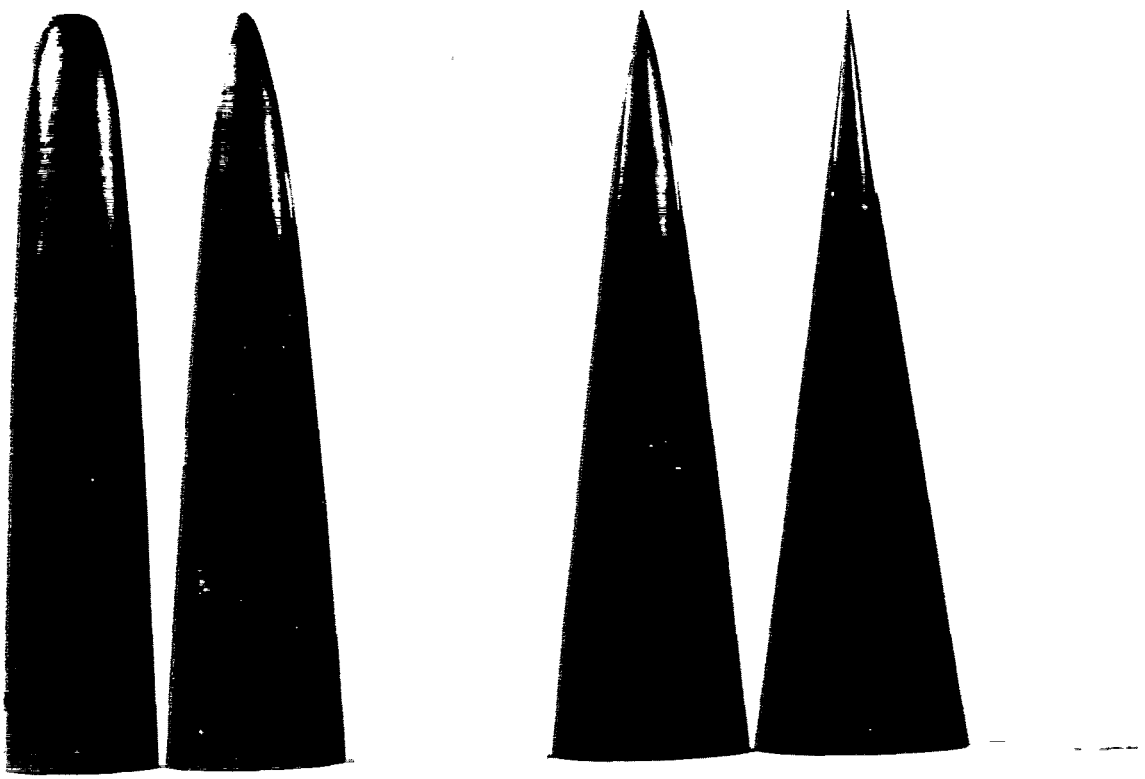

n = 0.25 n = 0.50 n = 0.66 n = 0.75 n = 1.00 Min. drag

(b) a/b = 2.0. L-65-2658

Figure 2.- Continued.

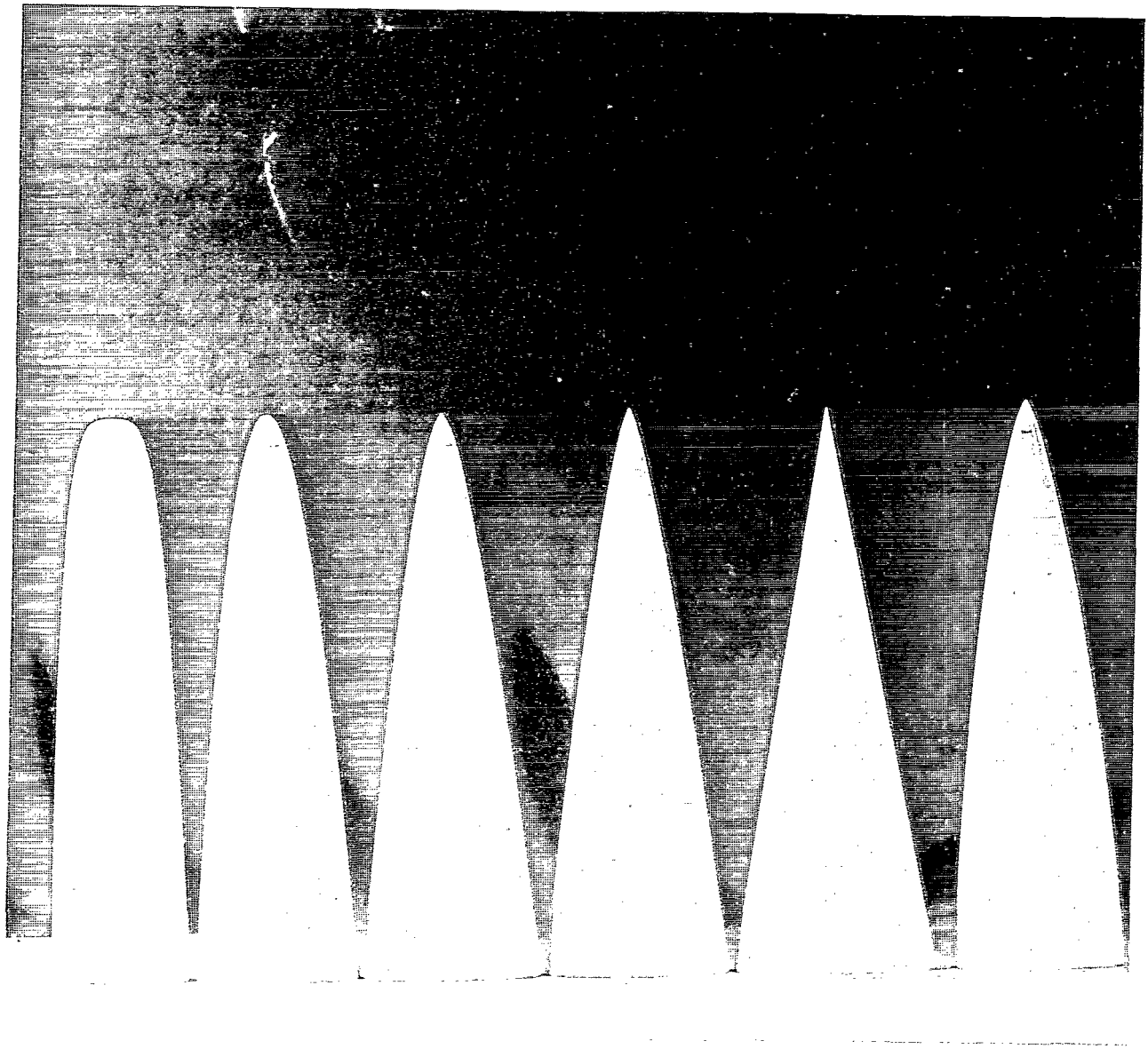

(c) a/b = 3.0. L-65-2659

Figure 2.- Continued.

L-65-690

a/b = 1.0 , n = 0.25

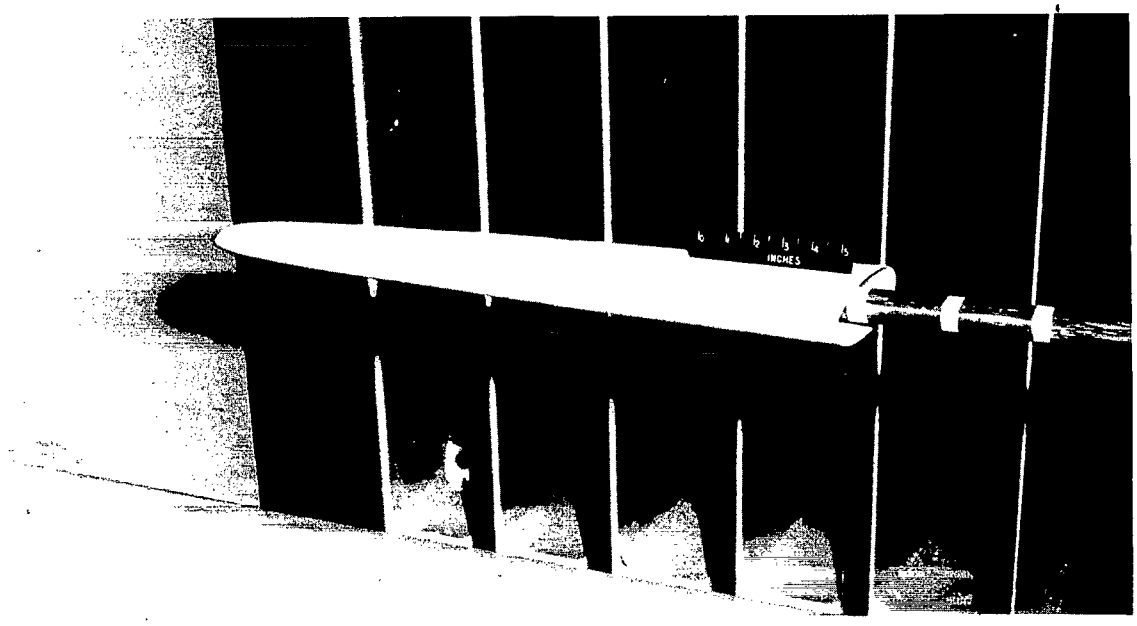

L-65-689

a/b = 3.0 , n = 0.25

(d) Two typical models mounted in the tunnel.

Figure 2.- Concluded.

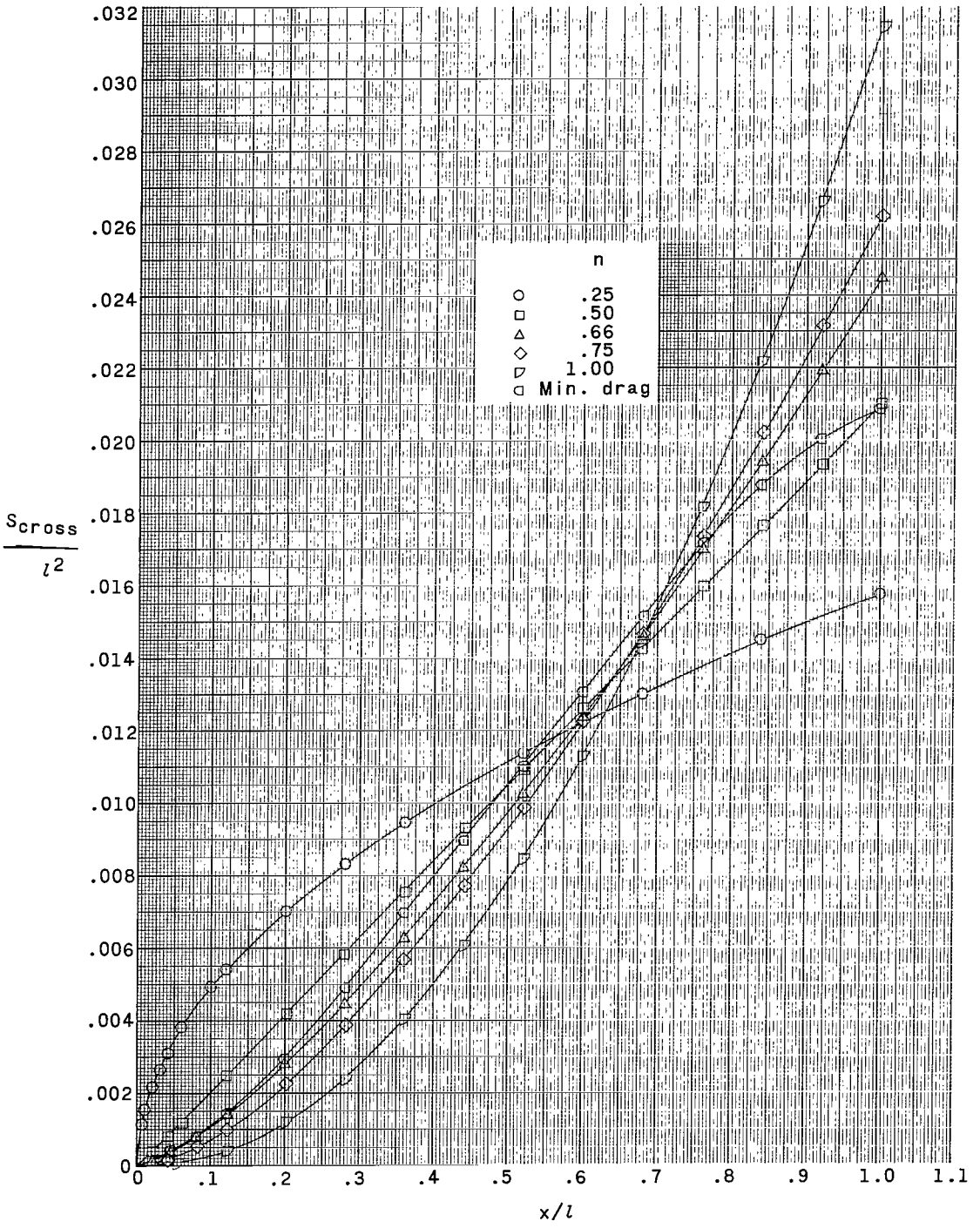

(a) Variation of S_{cross}/l^2 with x/l.

Figure 3.- Geometric characteristics of each of the bodies tested.

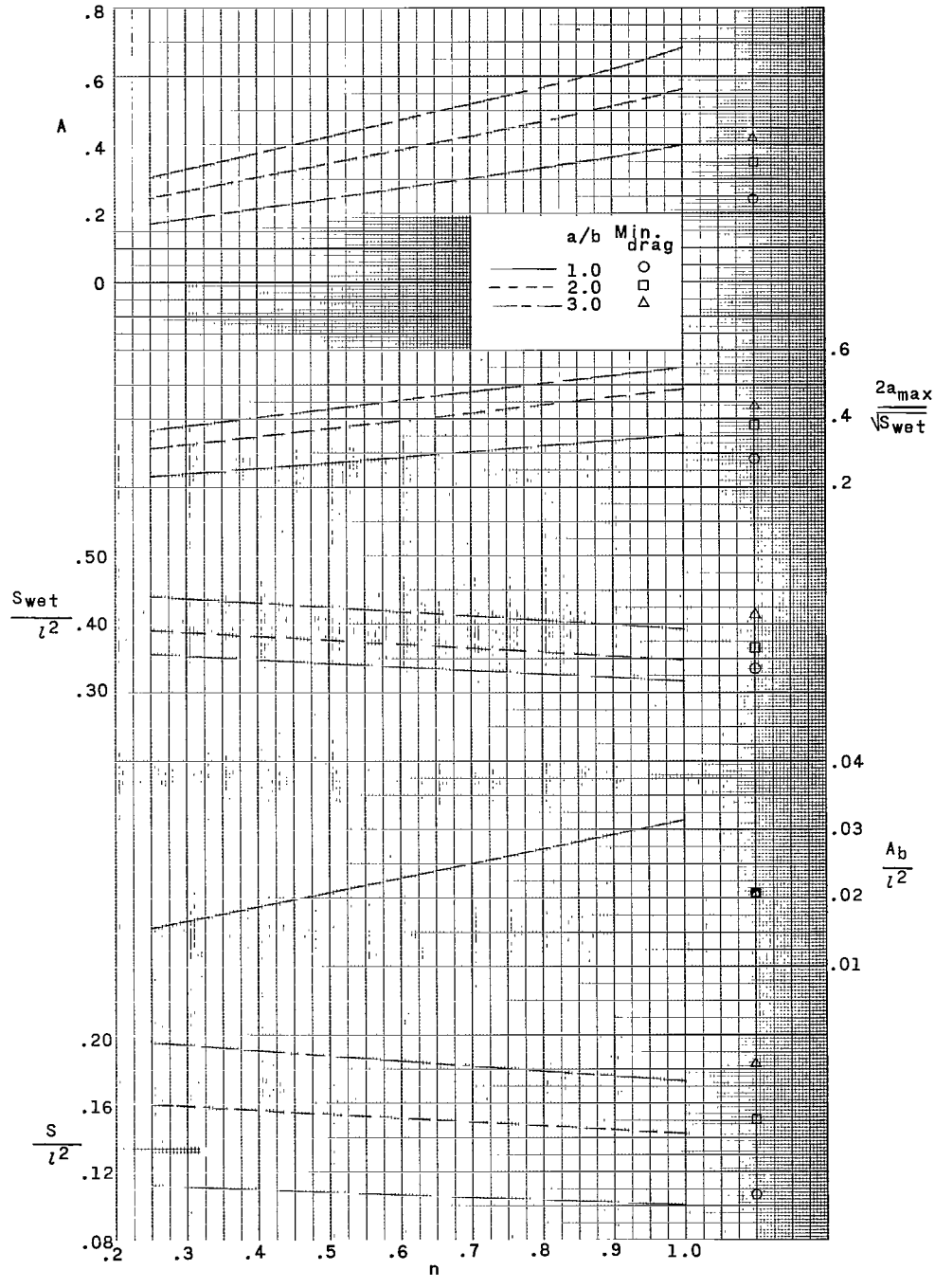

(b) Variation of various geometric parameters for each of the bodies, including the theoretical minimum-wave-drag body, with the power-body exponent n.

Figure 3.- Concluded.

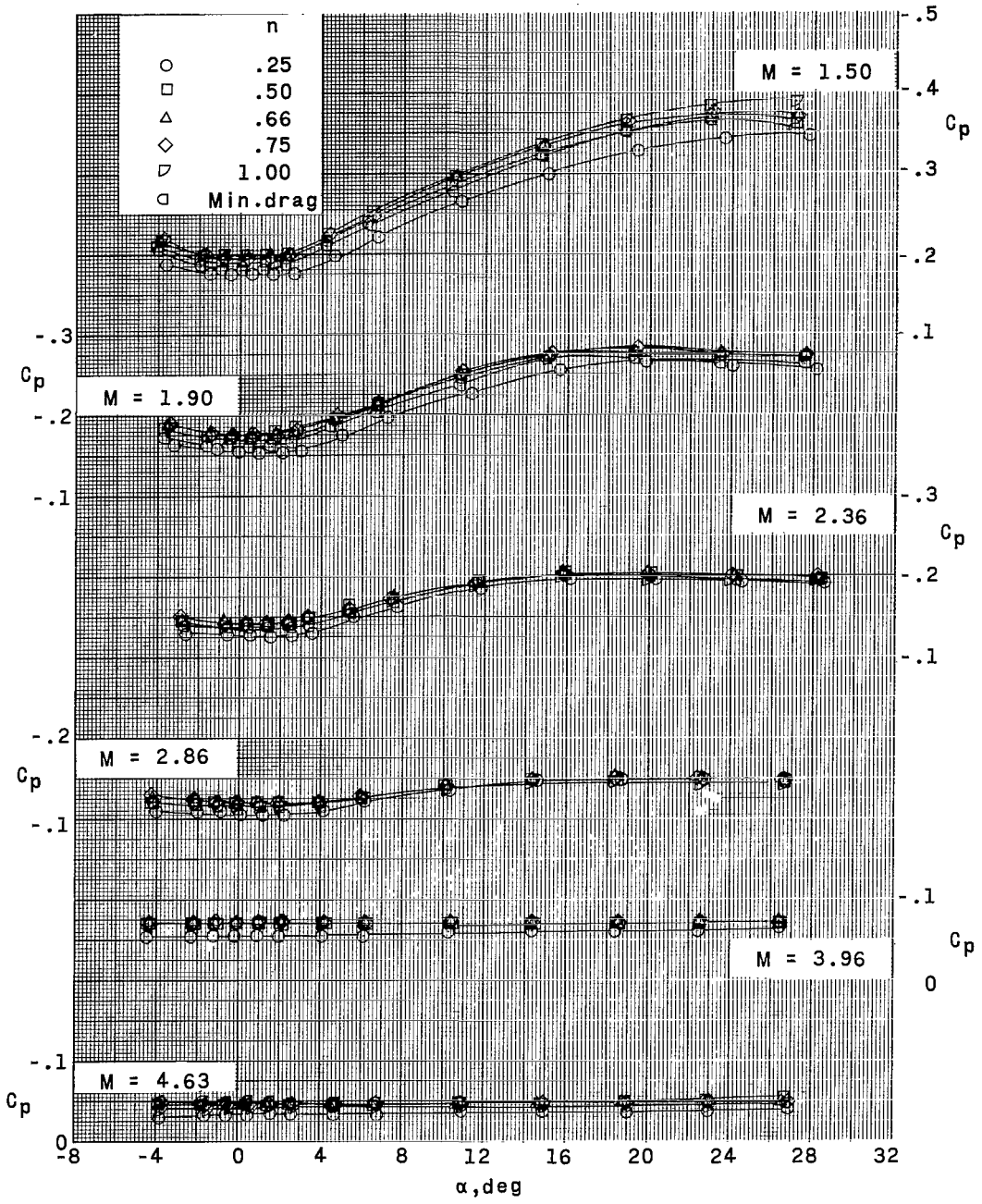

(a) a/b = 1.0.

Figure 4.- Variation of base pressure coefficient with angle of attack.

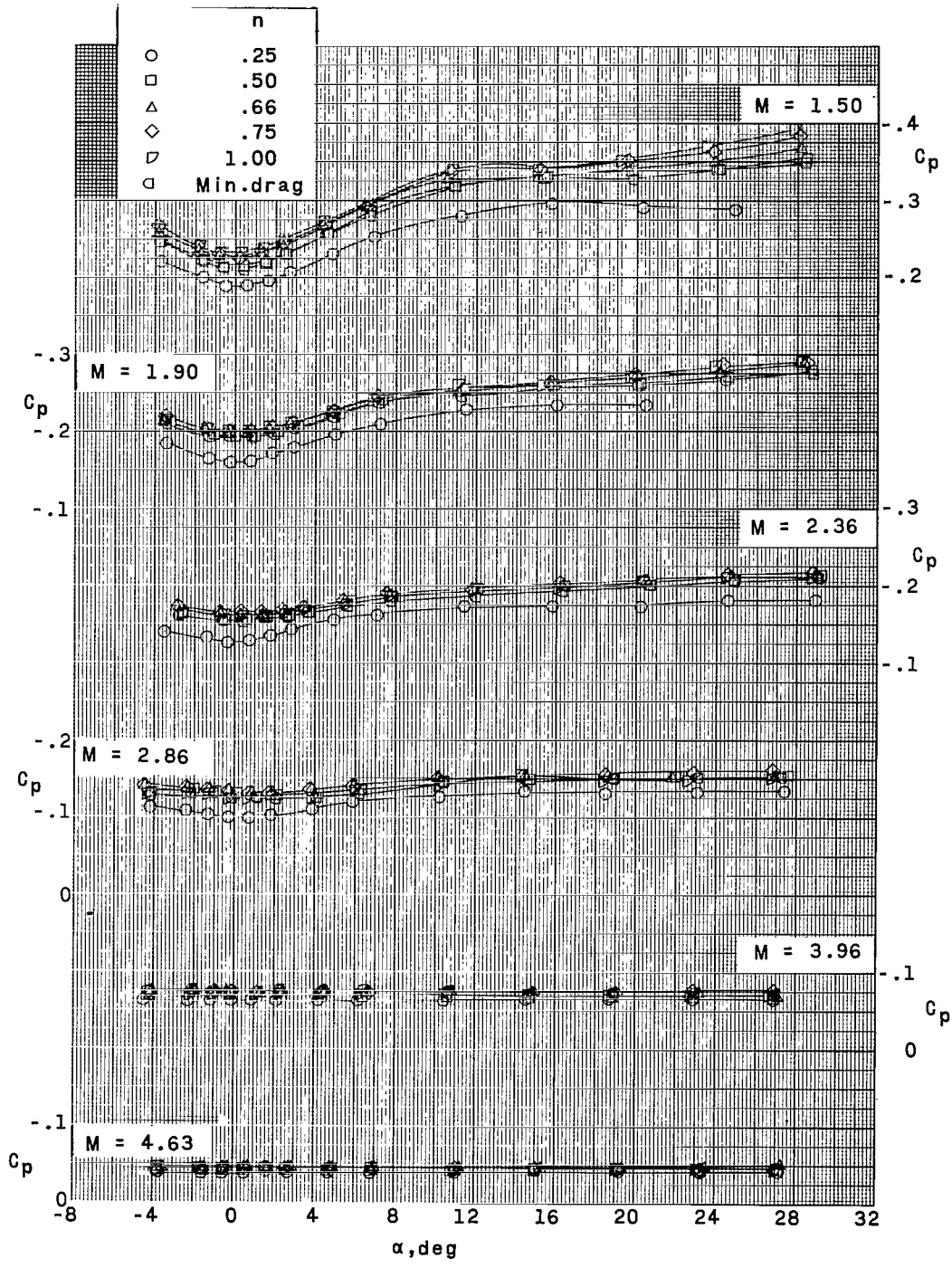

(b) a/b = 2.0.

Figure 4.- Continued.

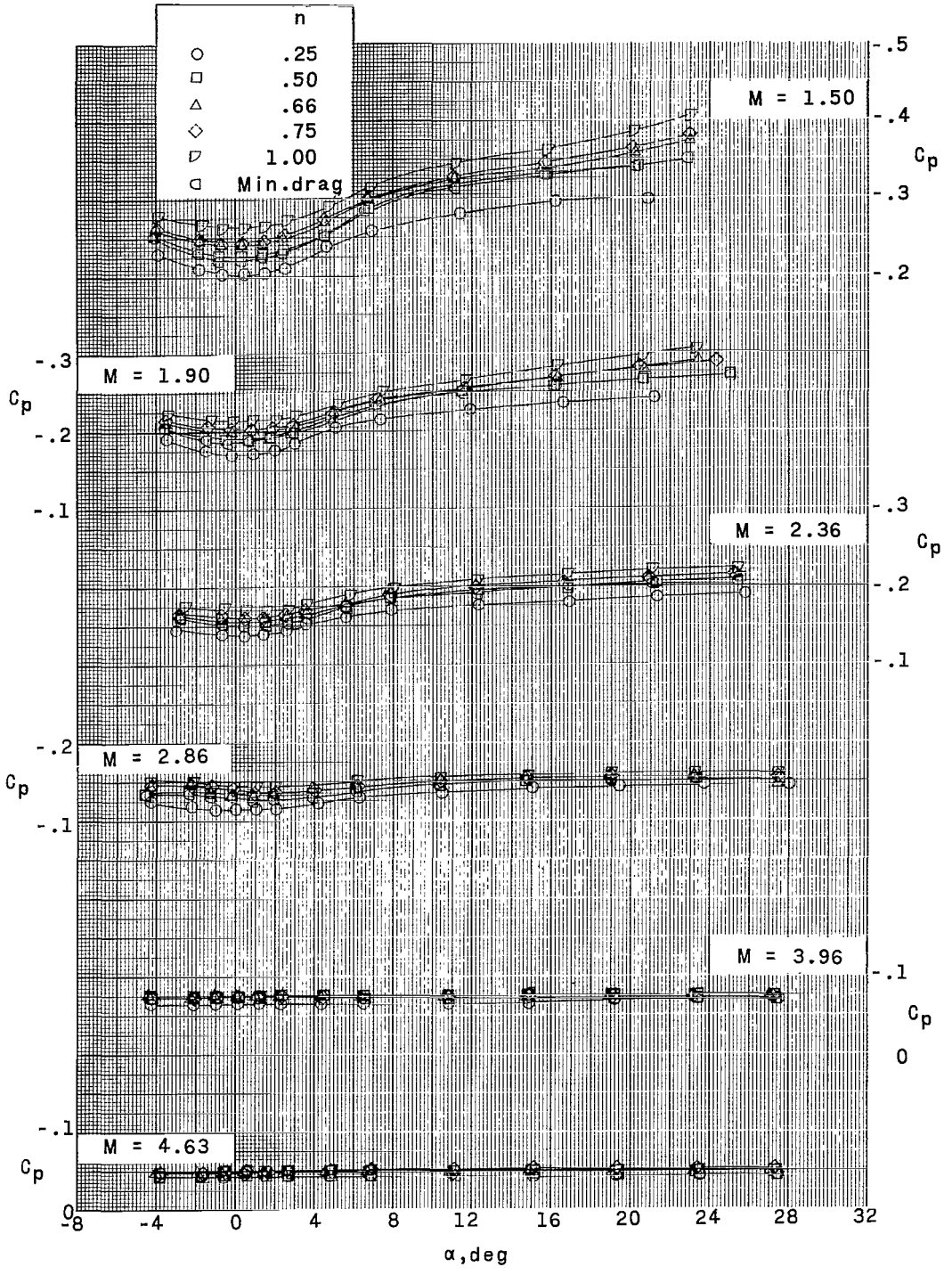

(c) a/b = 3.0.

Figure 4.- Concluded.

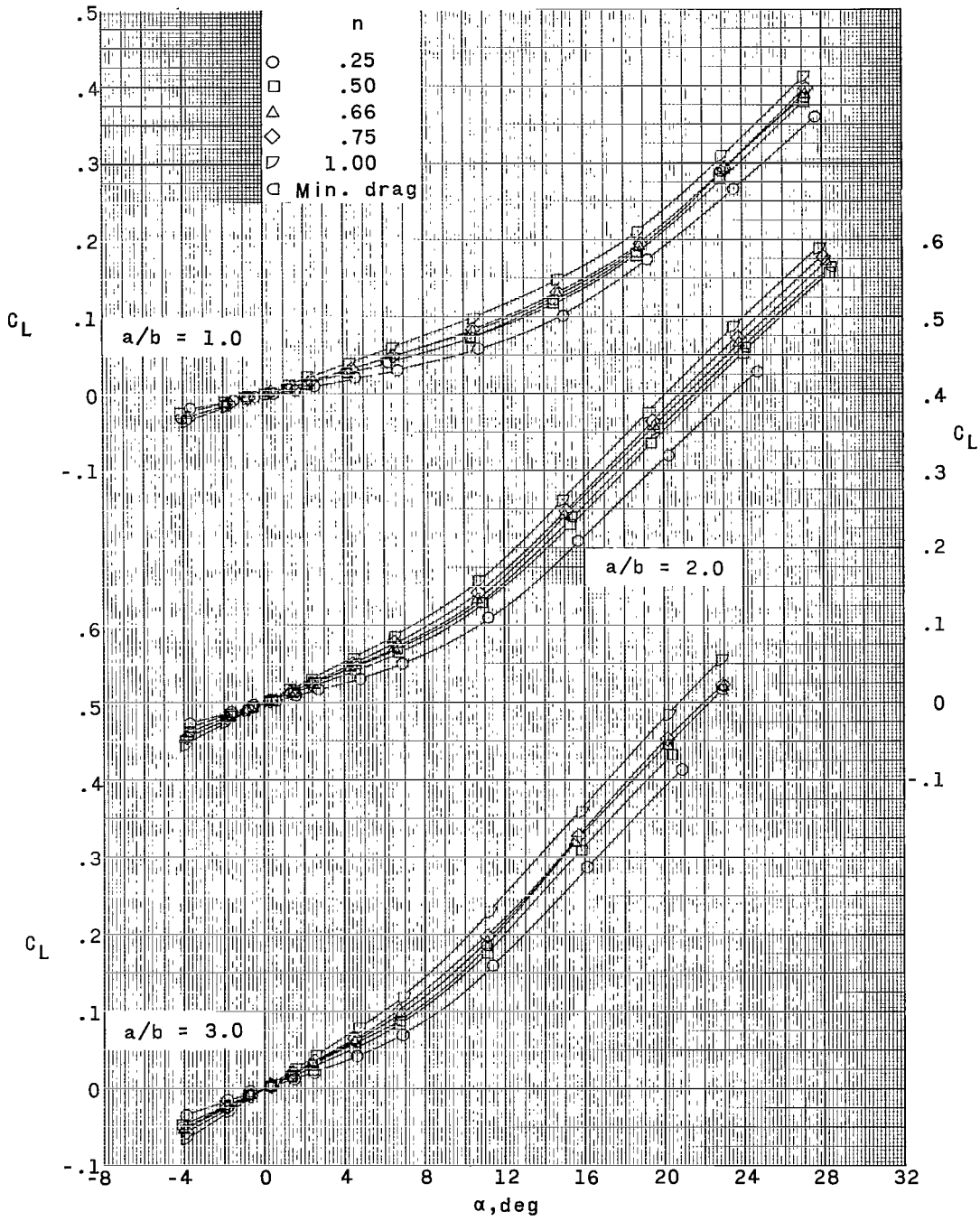

(a) C_L as a function of α.

Figure 5.- Longitudinal aerodynamic characteristics of power-law bodies and minimum-wave-drag body having variations in ellipticity at a Mach number of 1.50.

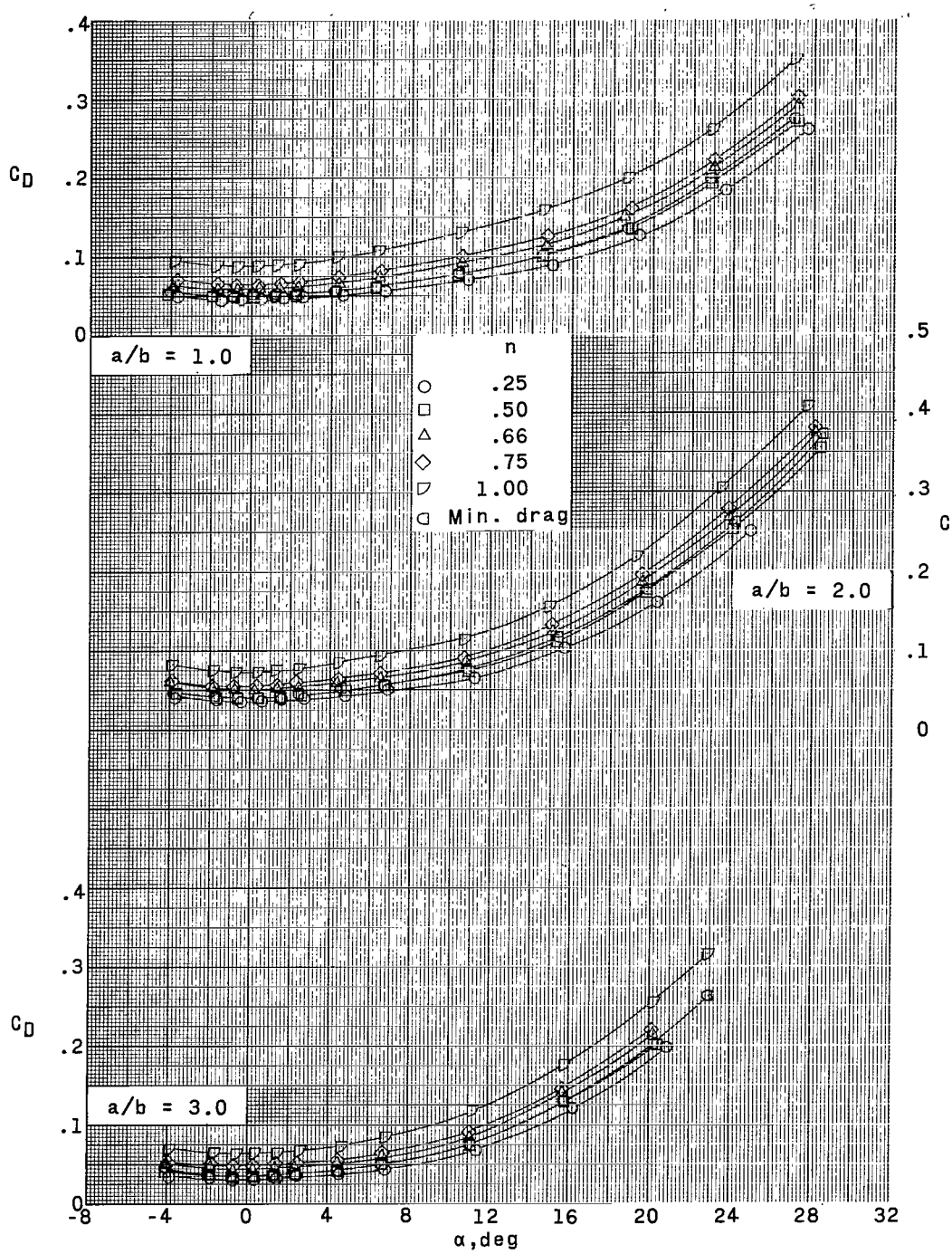

(b) C_D as a function of α.

Figure 5.- Continued.

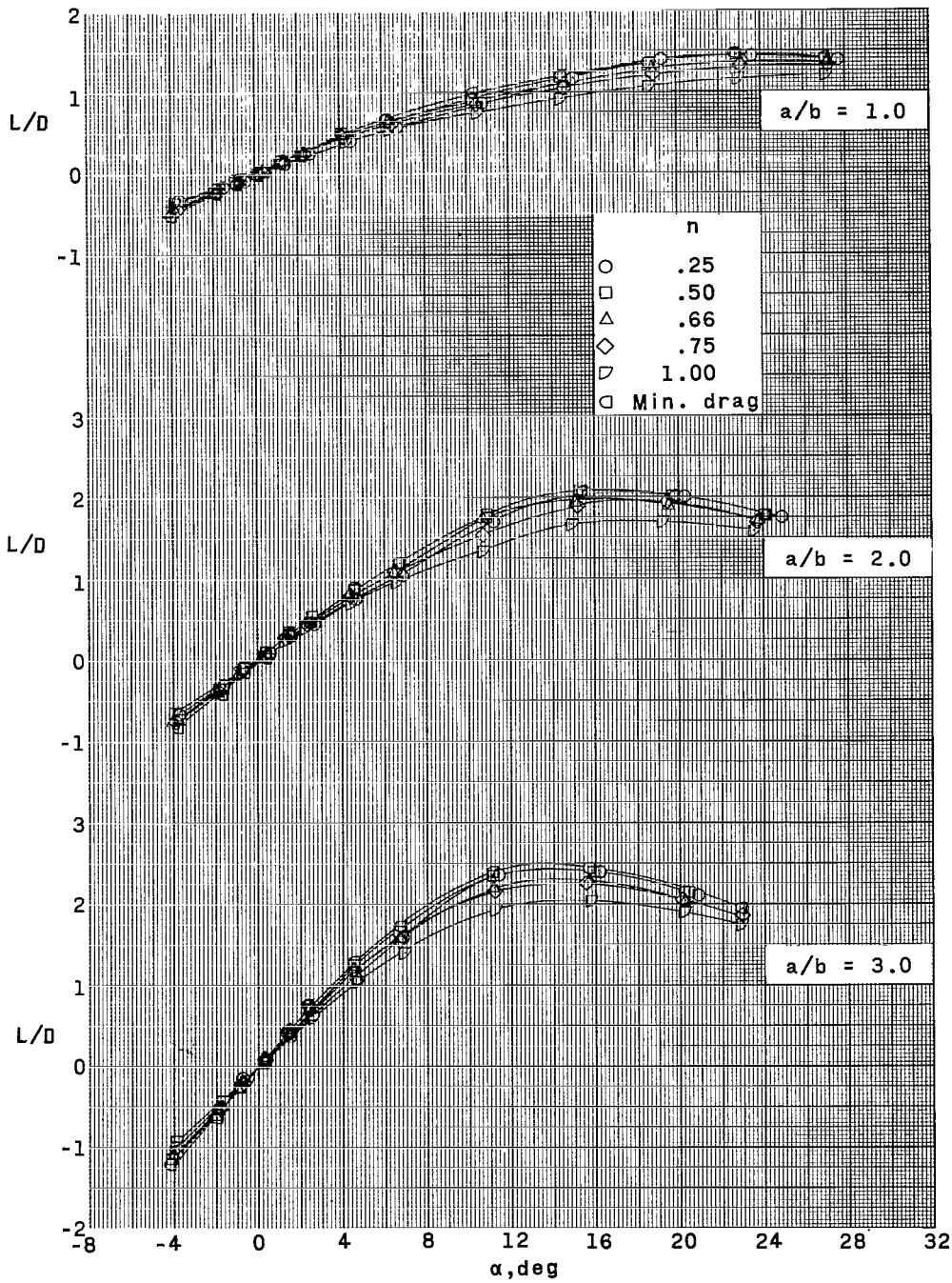

(c) L/D as a function of α.

Figure 5.- Continued.

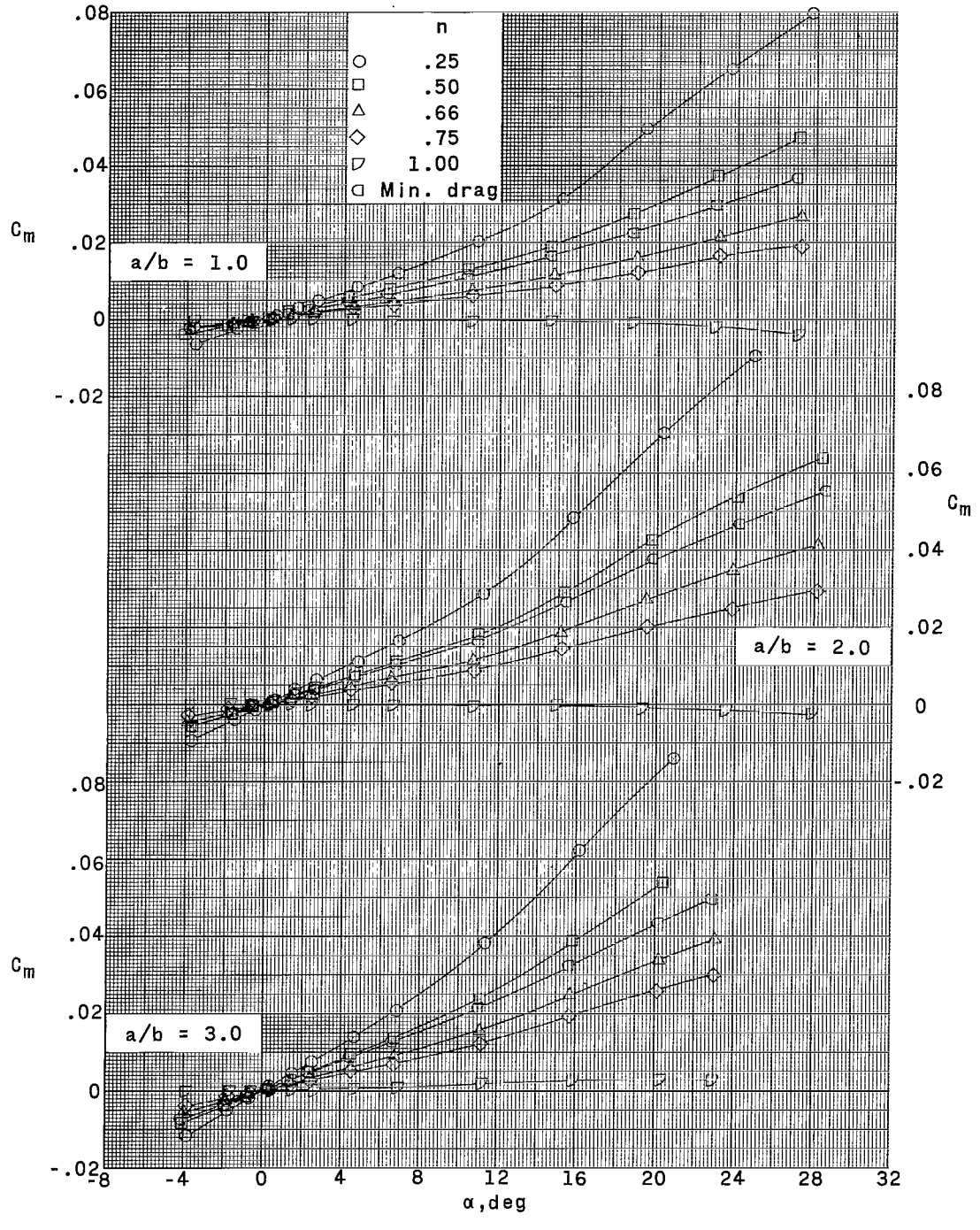

(d) C_m as a function of α.

Figure 5.- Concluded.

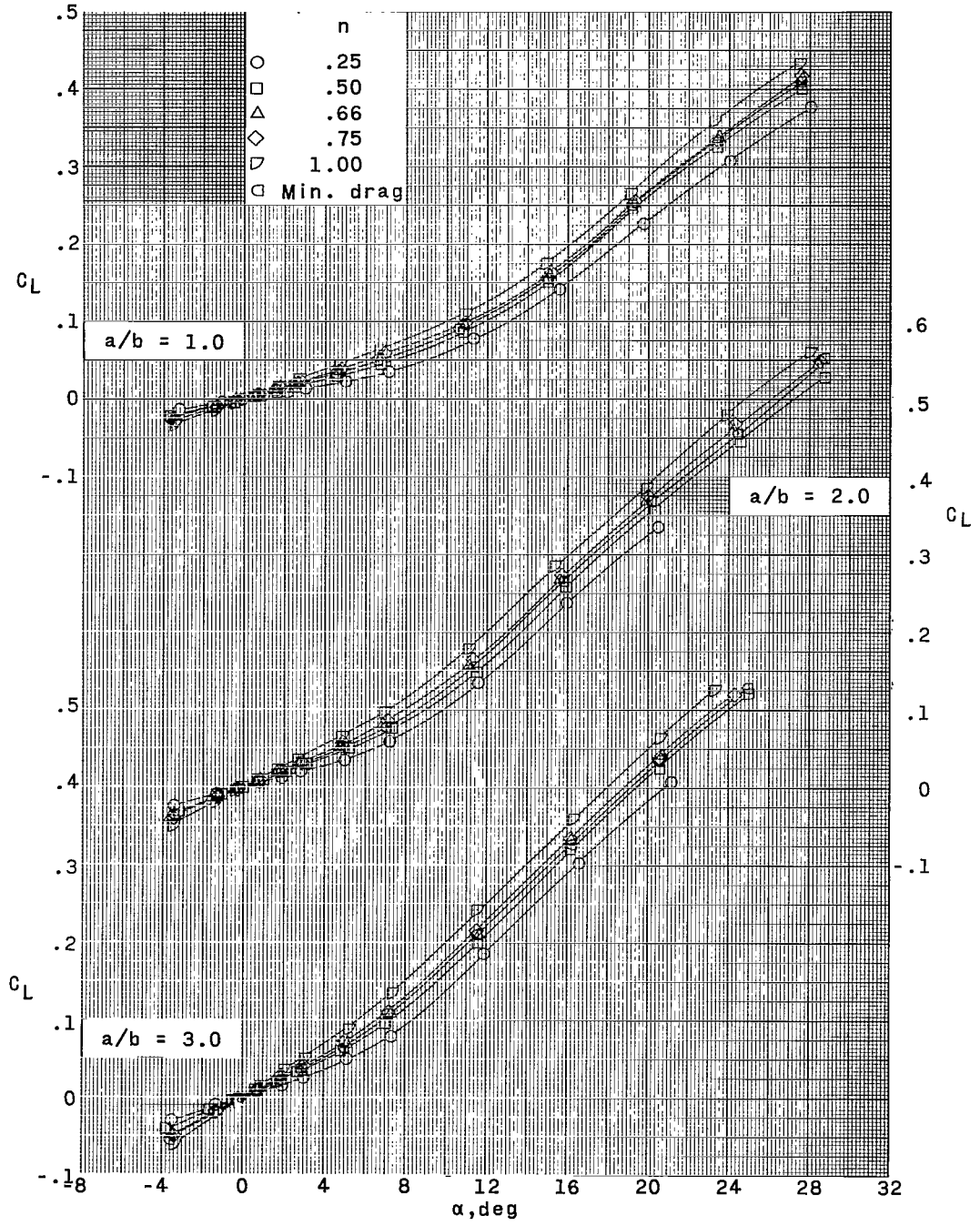

(a) C_L as a function of α.

Figure 6.- Longitudinal aerodynamic characteristic of power-law bodies and minimum-wave-drag body having variations in ellipticity at a Mach number of 1.90.

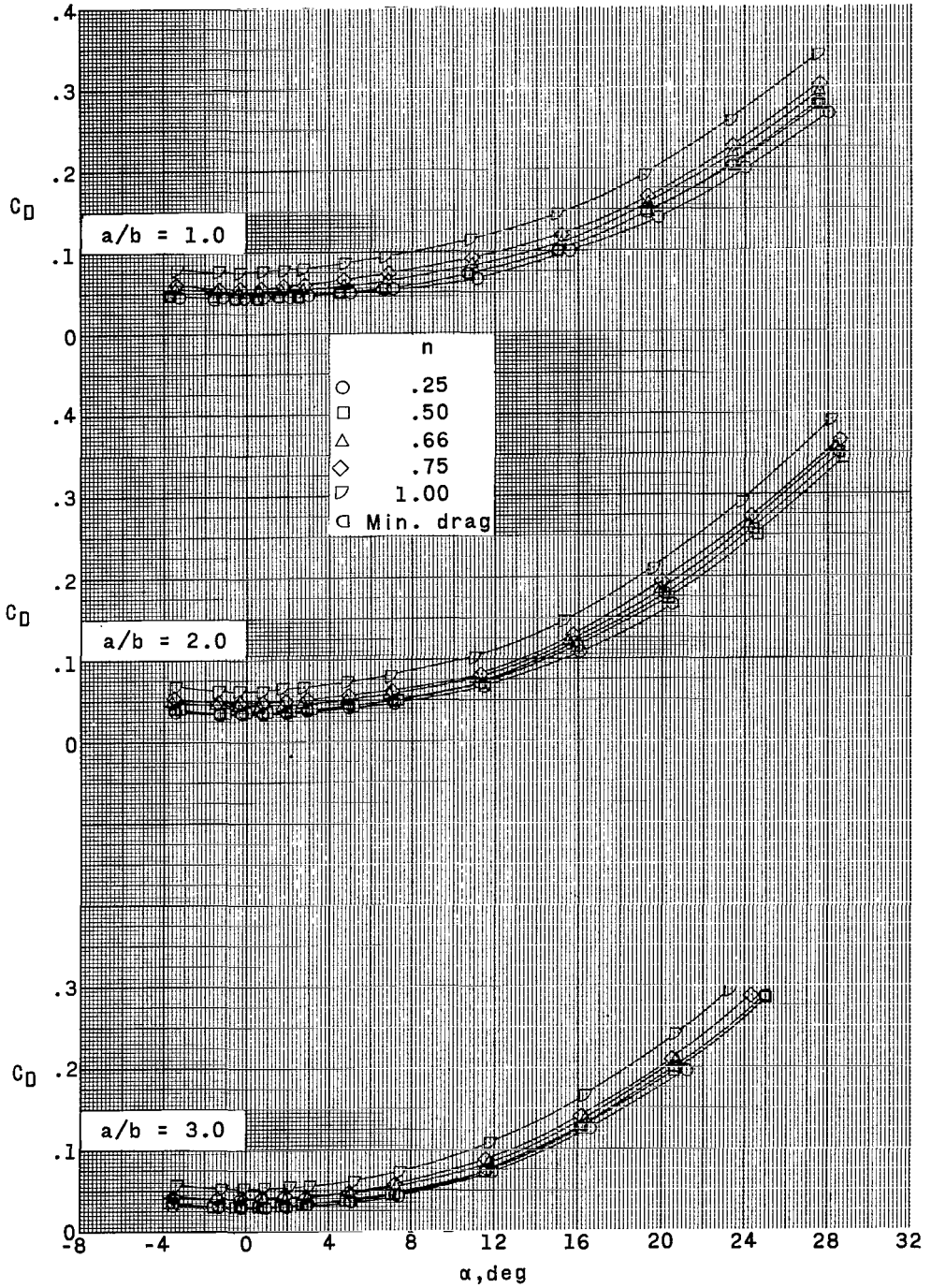

(b) C_D as a function of α.

Figure 6.- Continued.

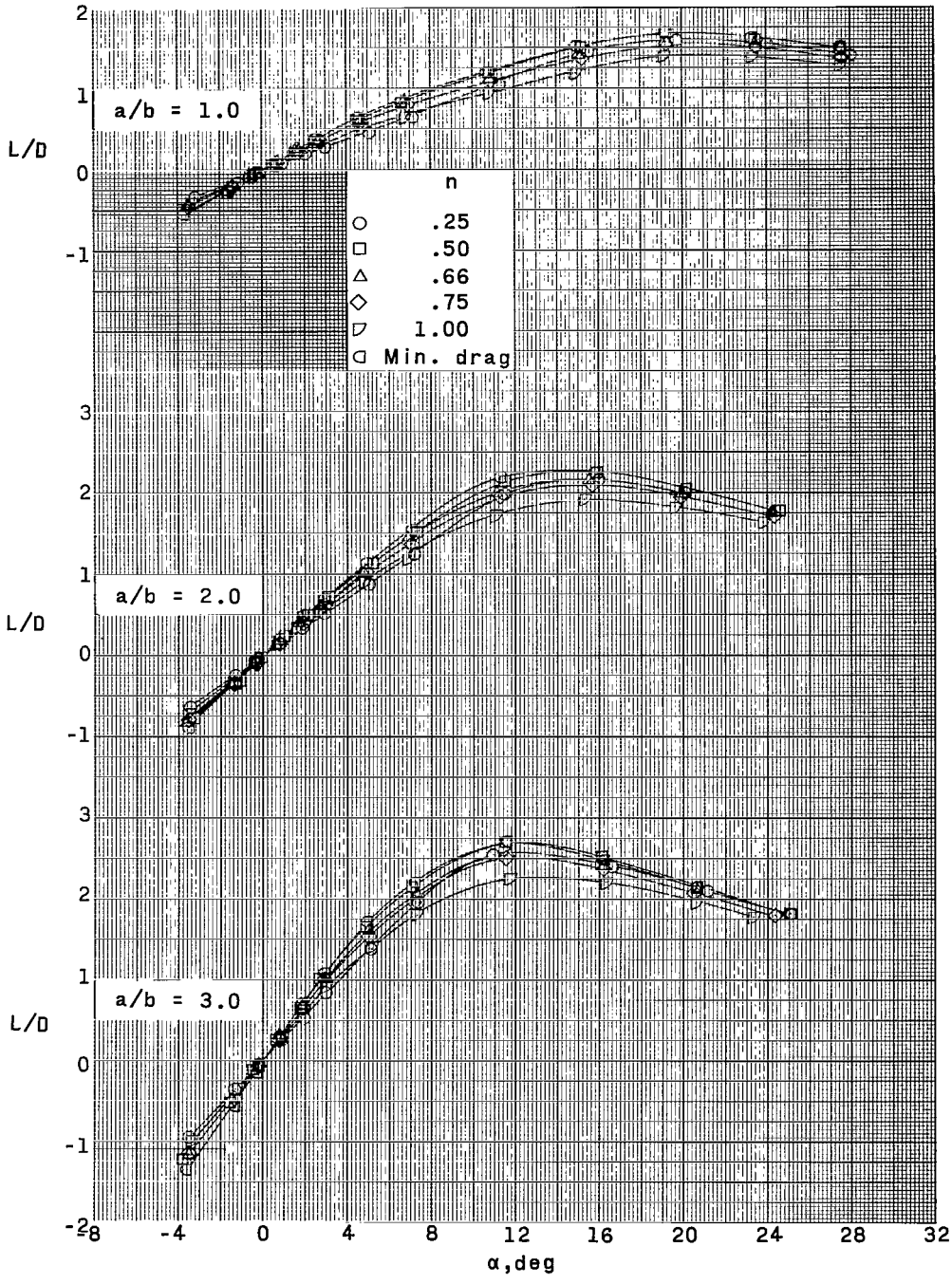

(c) L/D as a function of α.

Figure 6.- Continued.

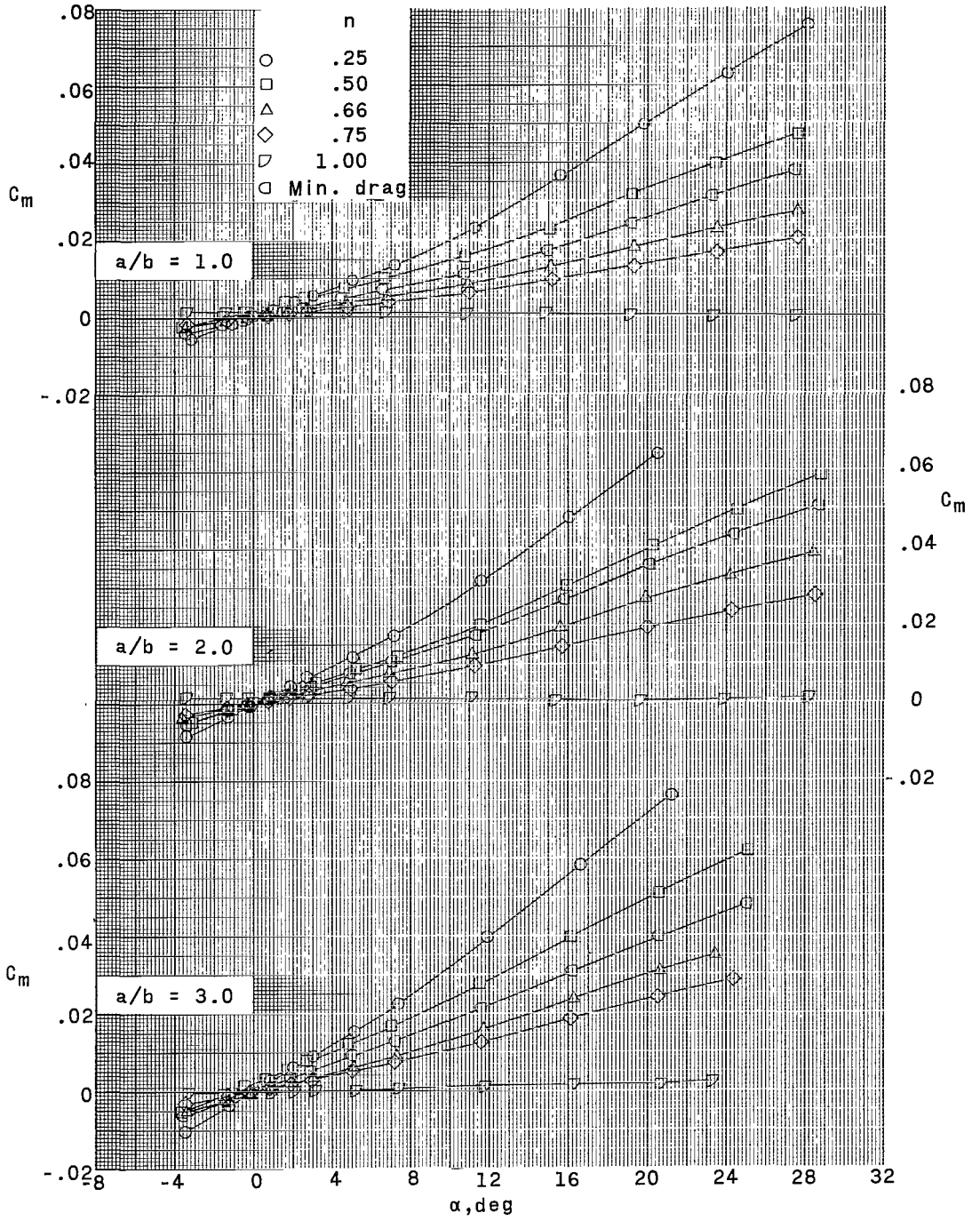

(d) C_m as a function of α.

Figure 6.- Concluded.

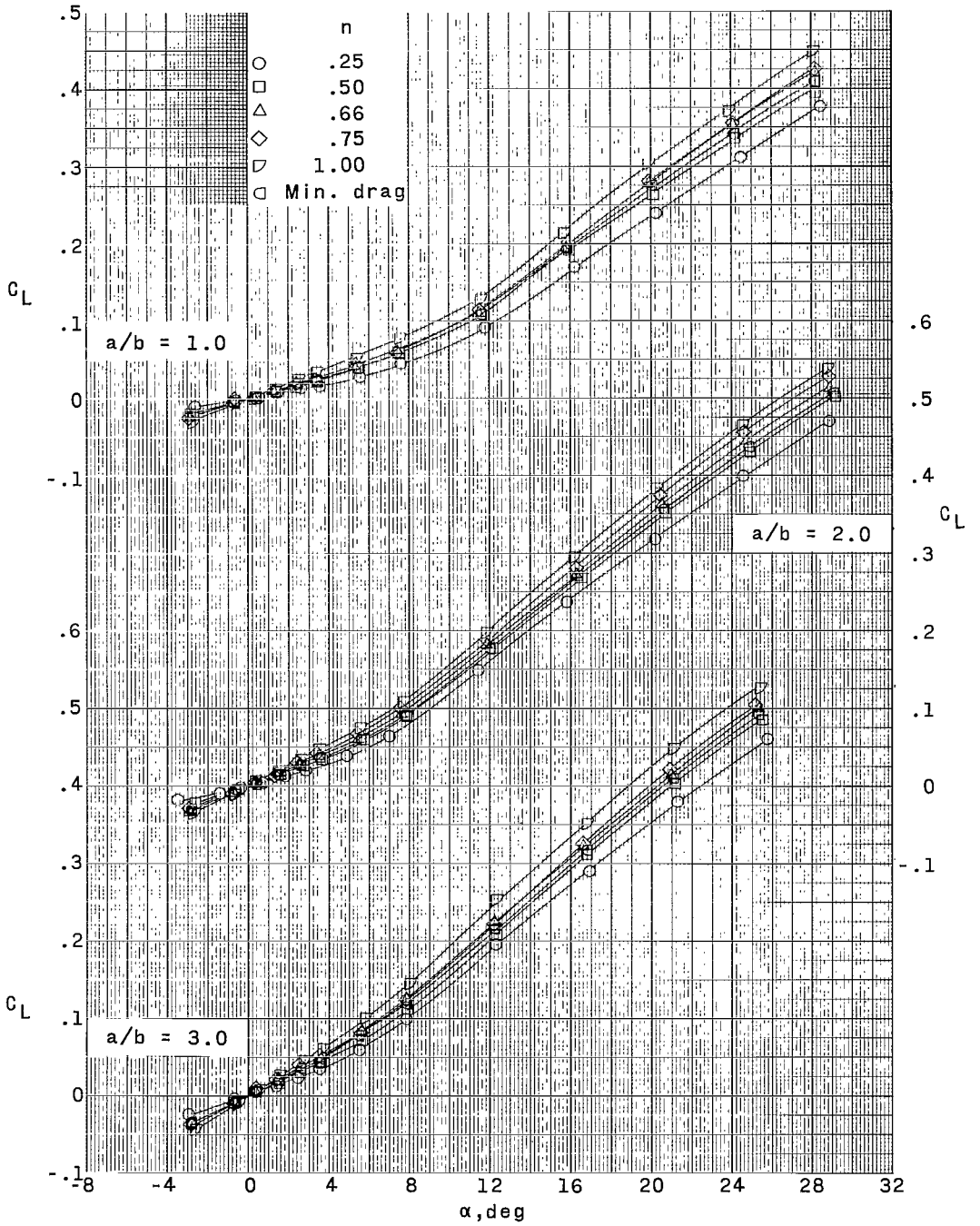

(a) C_L as a function of α.

Figure 7.- Longitudinal aerodynamic characteristics of power-law bodies and minimum-wave-drag body having variations in ellipticity at a Mach number of 2.36.

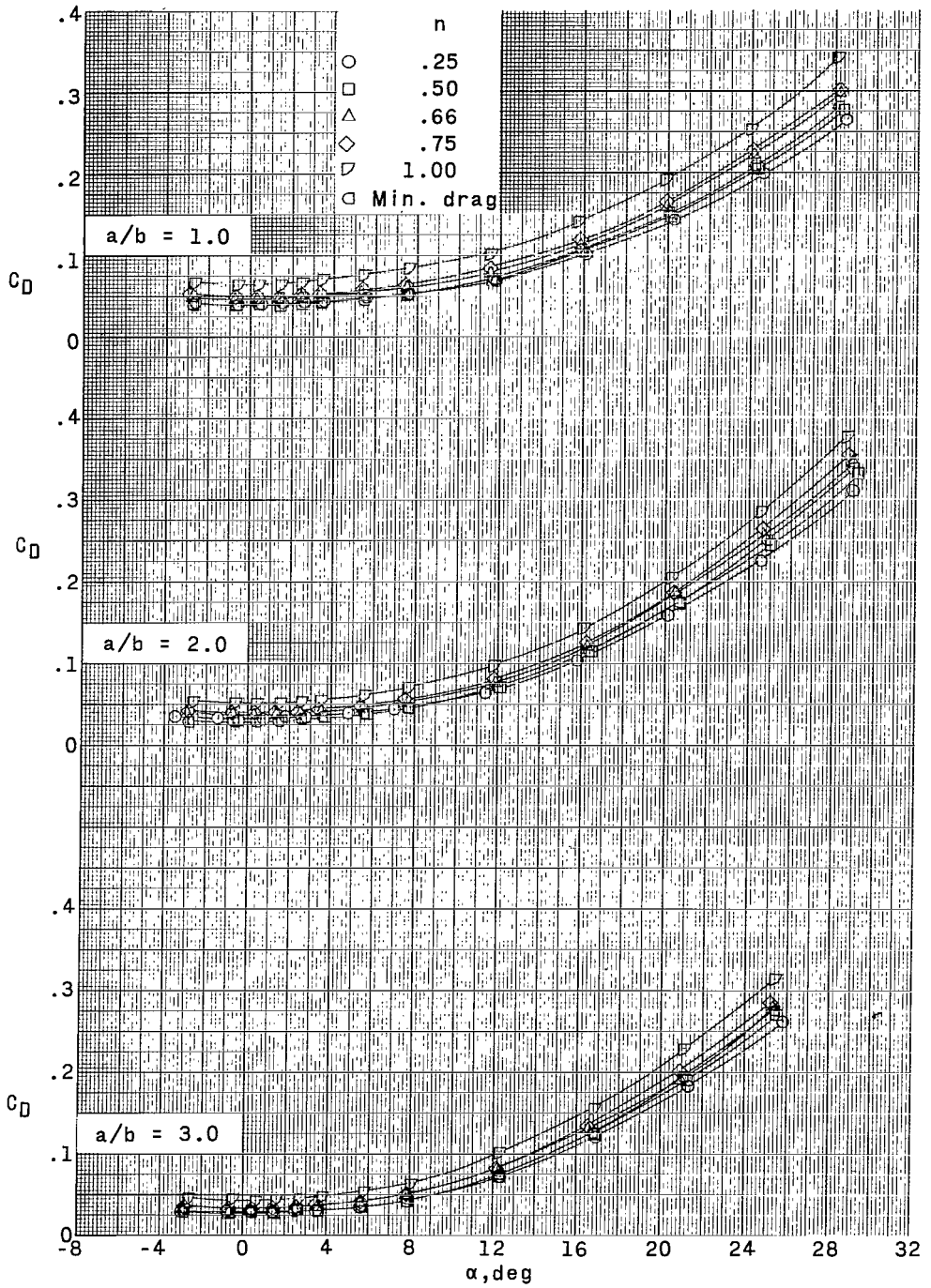

(b) C_D as a function of α.

Figure 7.- Continued.

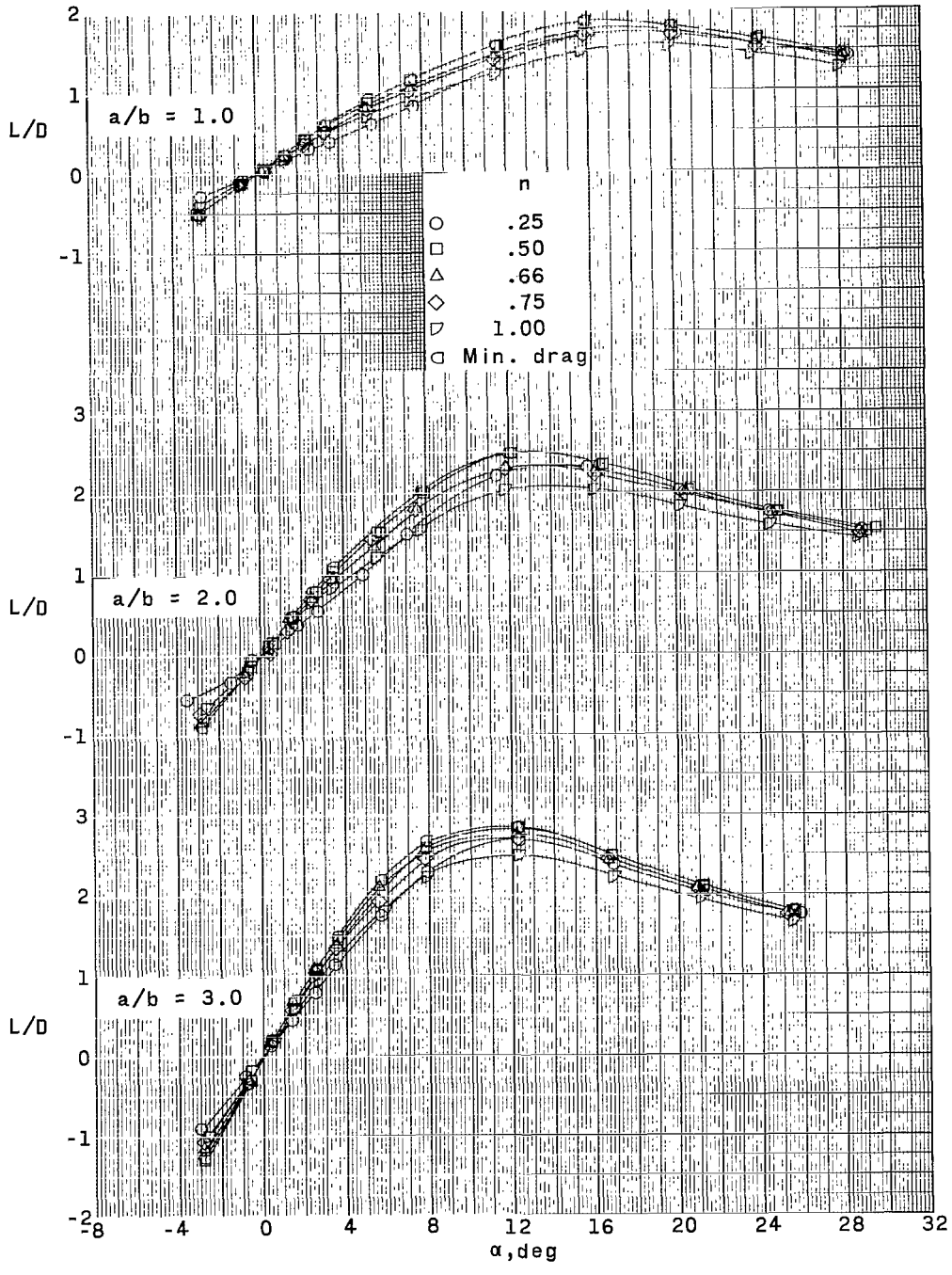

(c) L/D as a function of α.

Figure 7.- Continued.

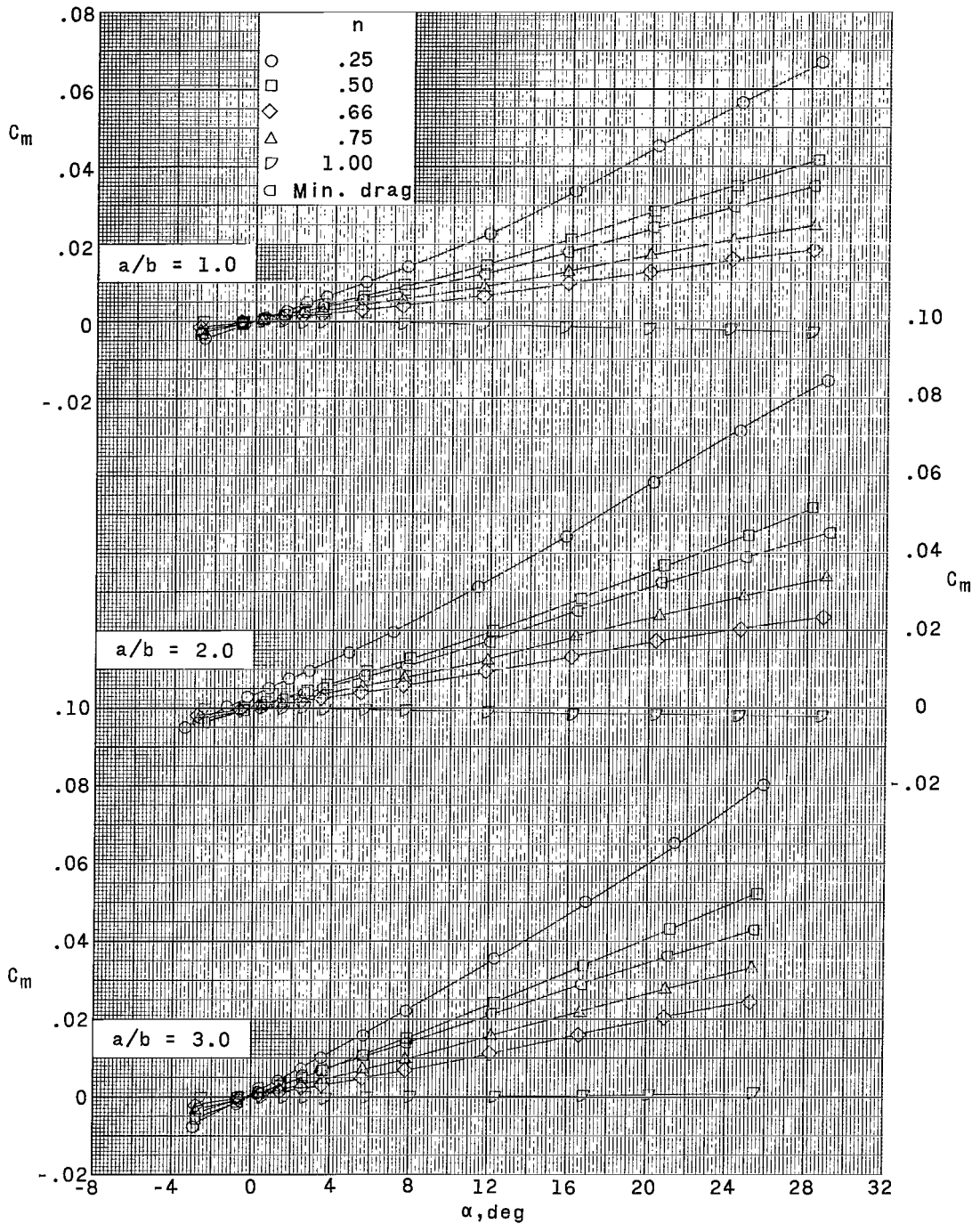

(d) C_m as a function of α.

Figure 7.- Concluded.

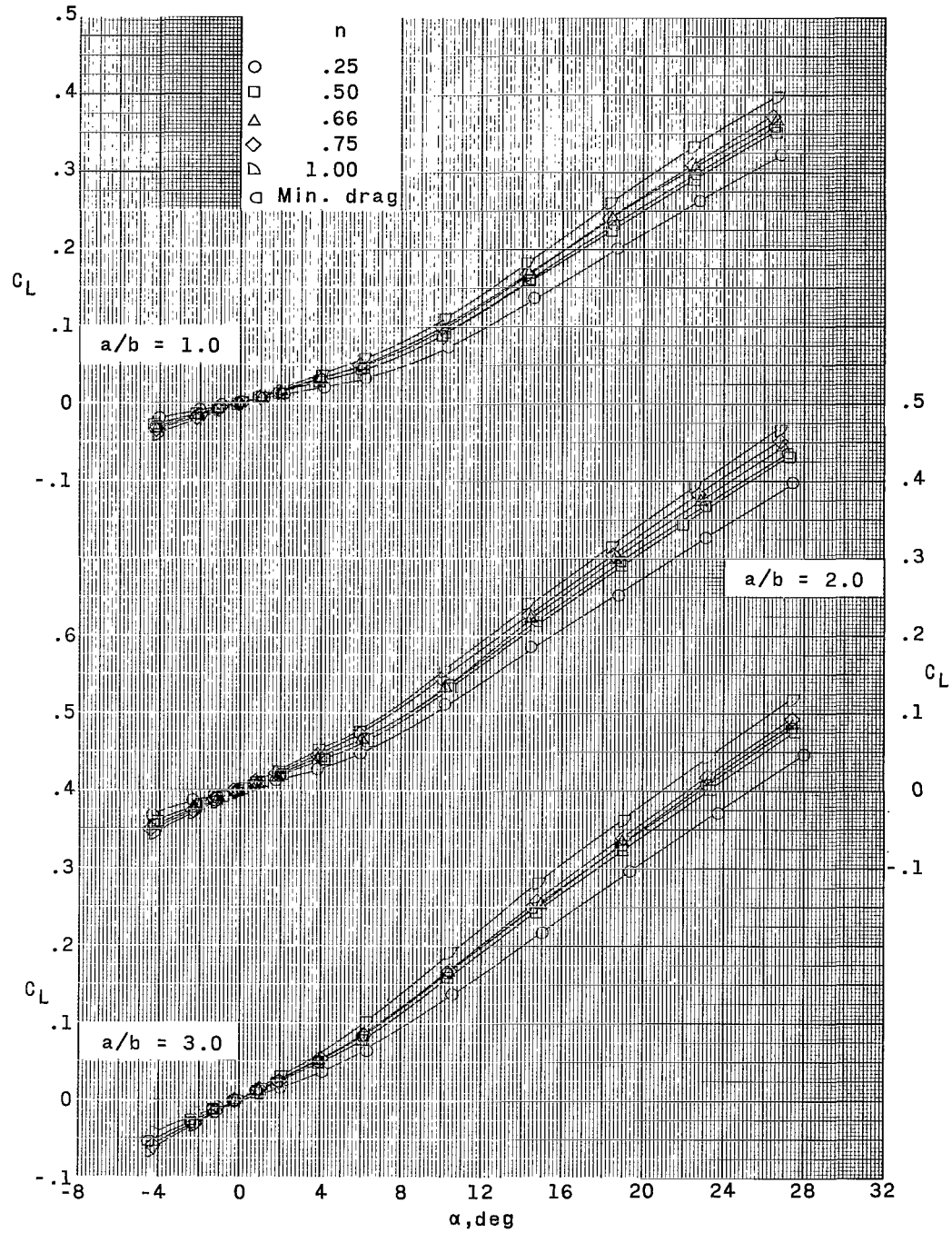

(a) C_L as a function of α.

Figure 8.- Longitudinal aerodynamic characteristics of power-law bodies and minimum-wave-drag body having variations in ellipticity at a Mach number of 2.86.

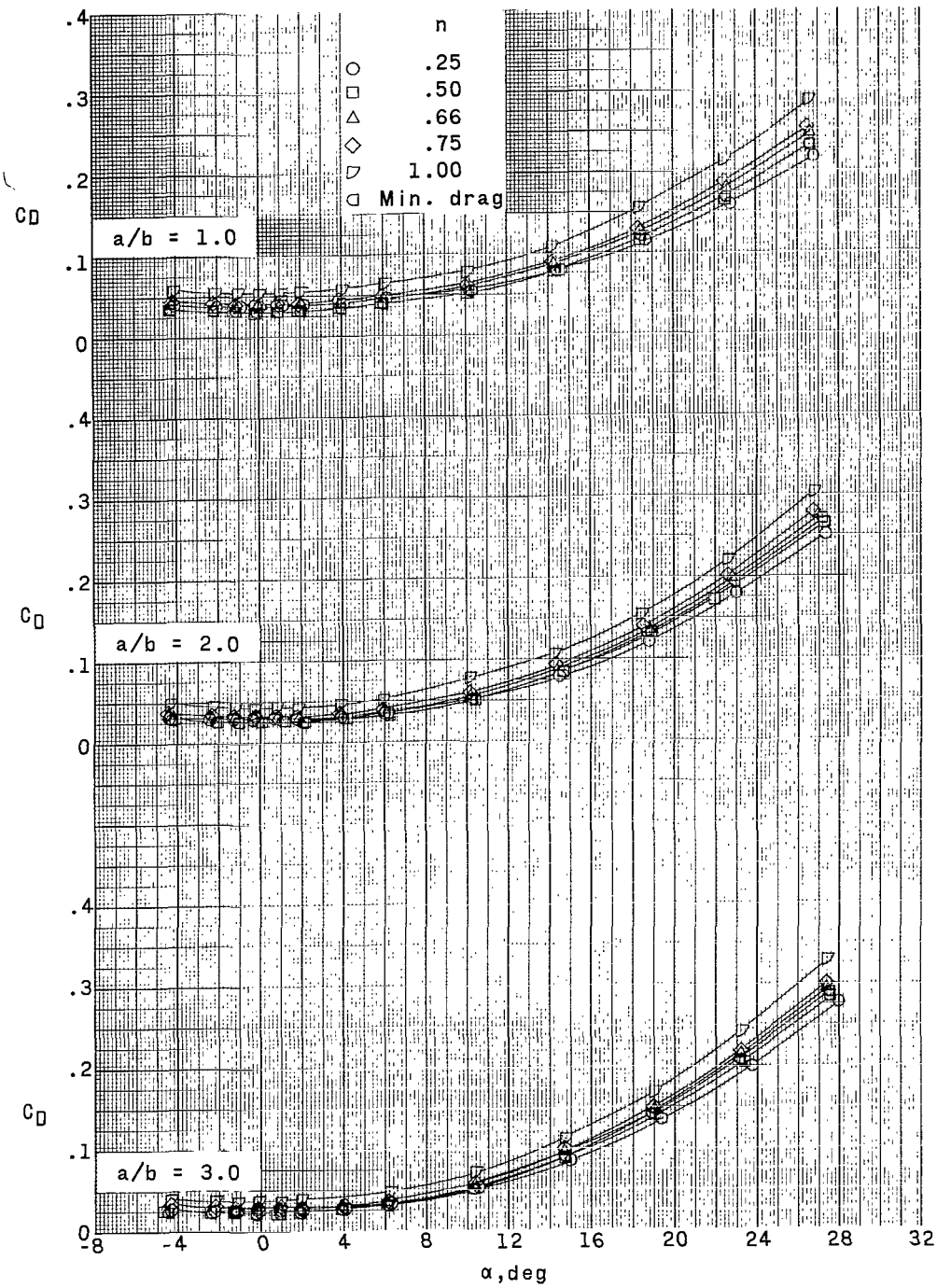

(b) C_D as a function of α.

Figure 8.- Continued.

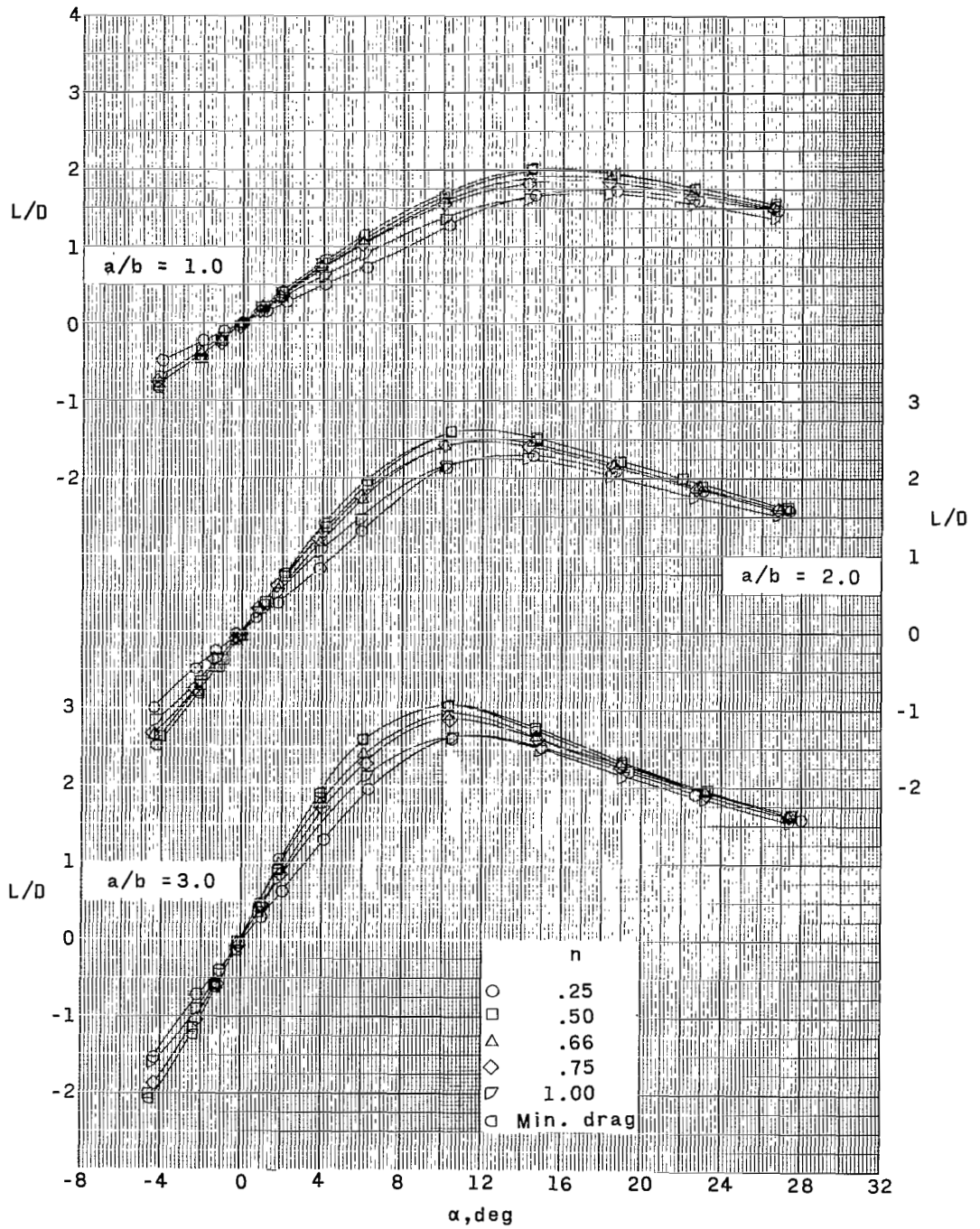

(c) L/D as a function of α.

Figure 8.- Continued.

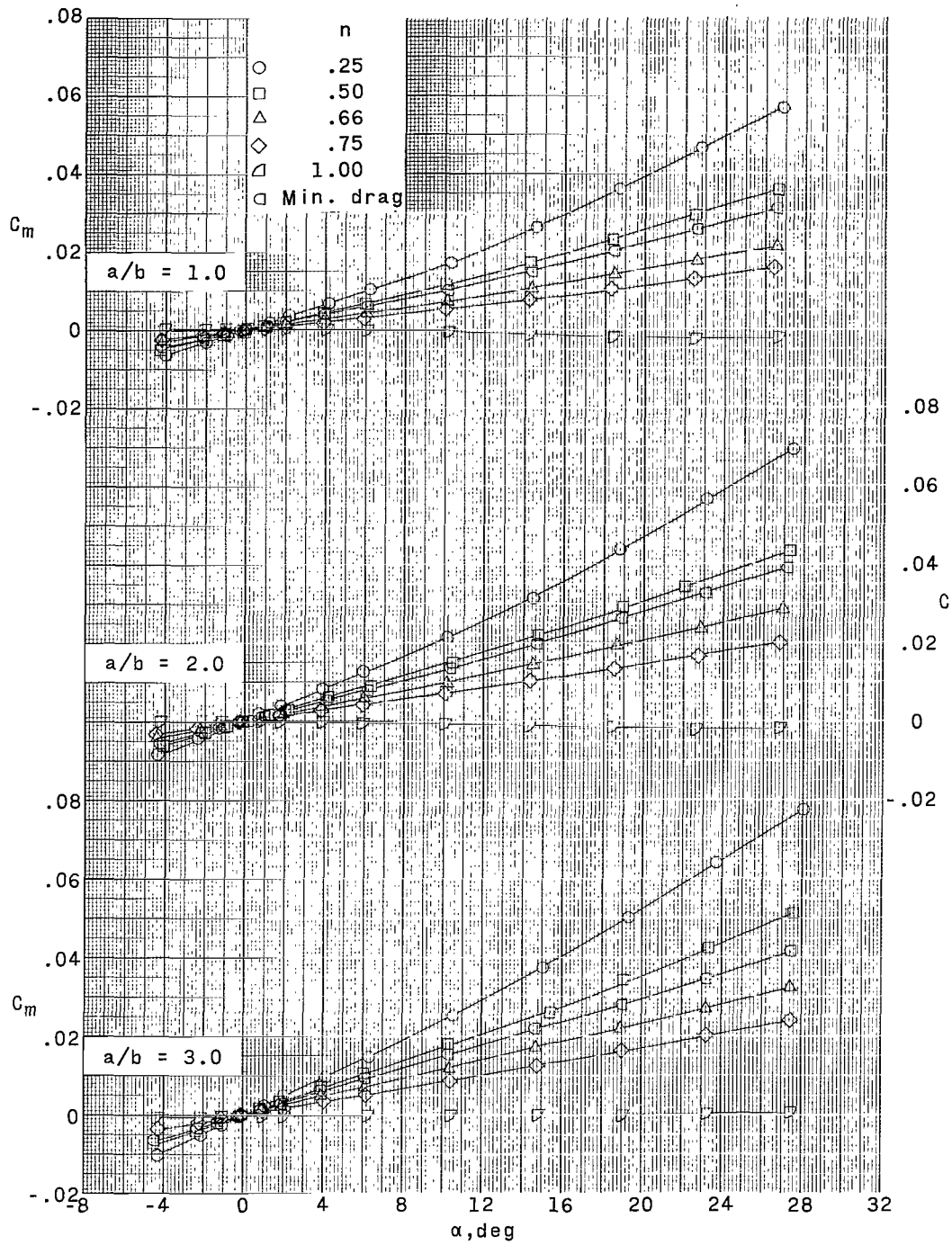

(d) C_m as a function of α.

Figure 8.- Concluded.

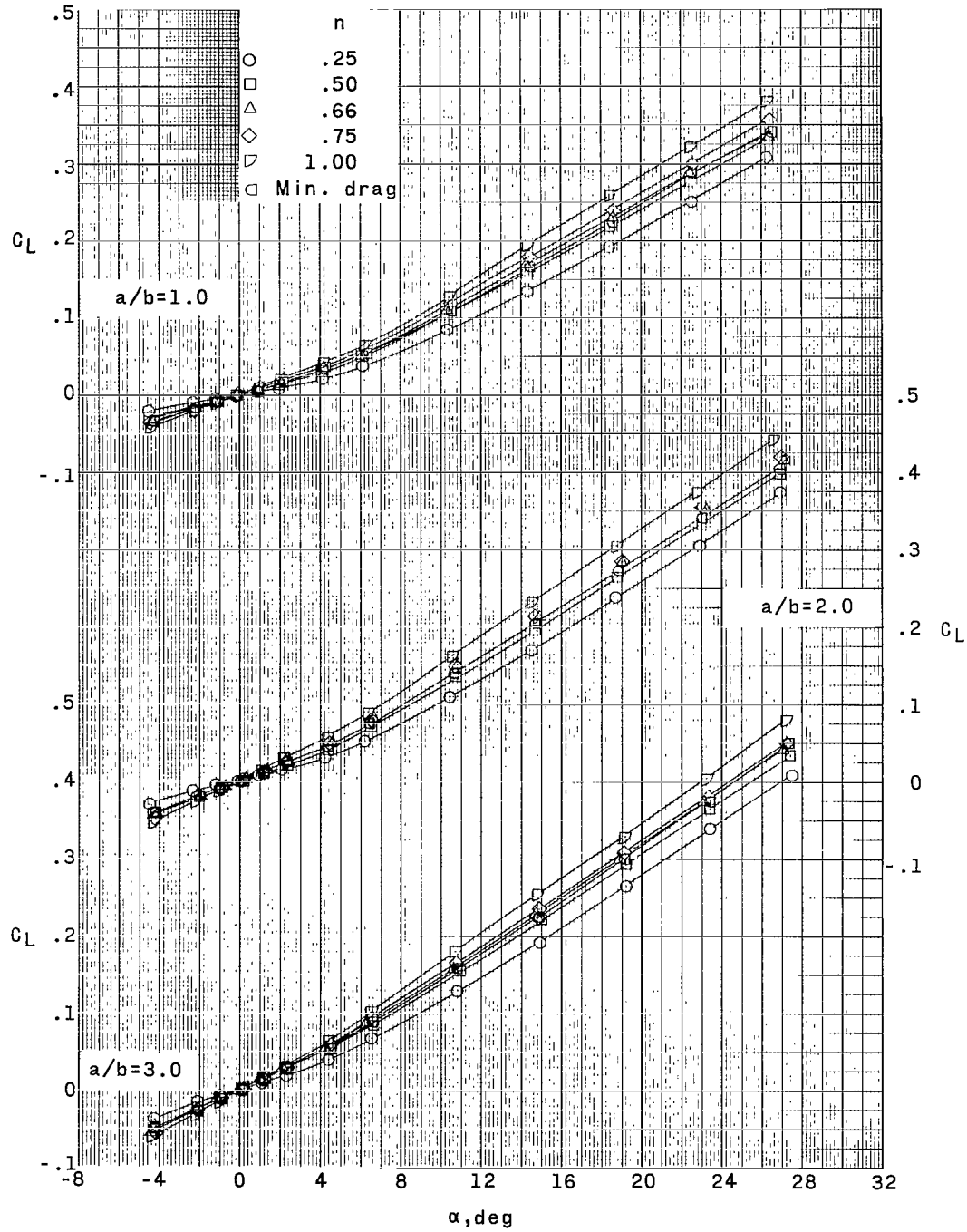

(a) C_L as a function of α.

Figure 9.- Longitudinal aerodynamic characteristics of power-law bodies and minimum-wave-drag body having variations in ellipticity at a Mach number of 3.96.

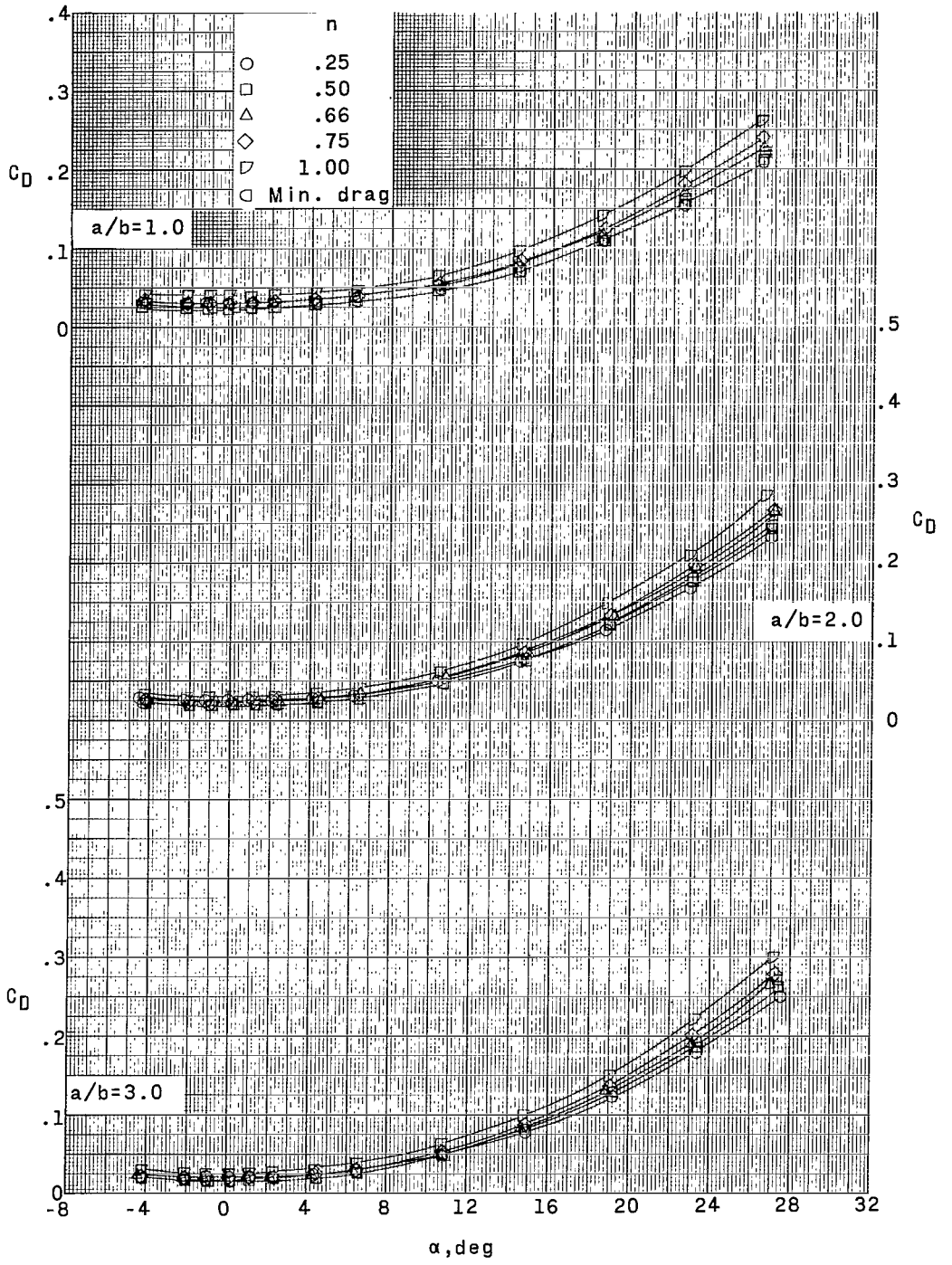

(b) C_D as a function of α.

Figure 9.- Continued.

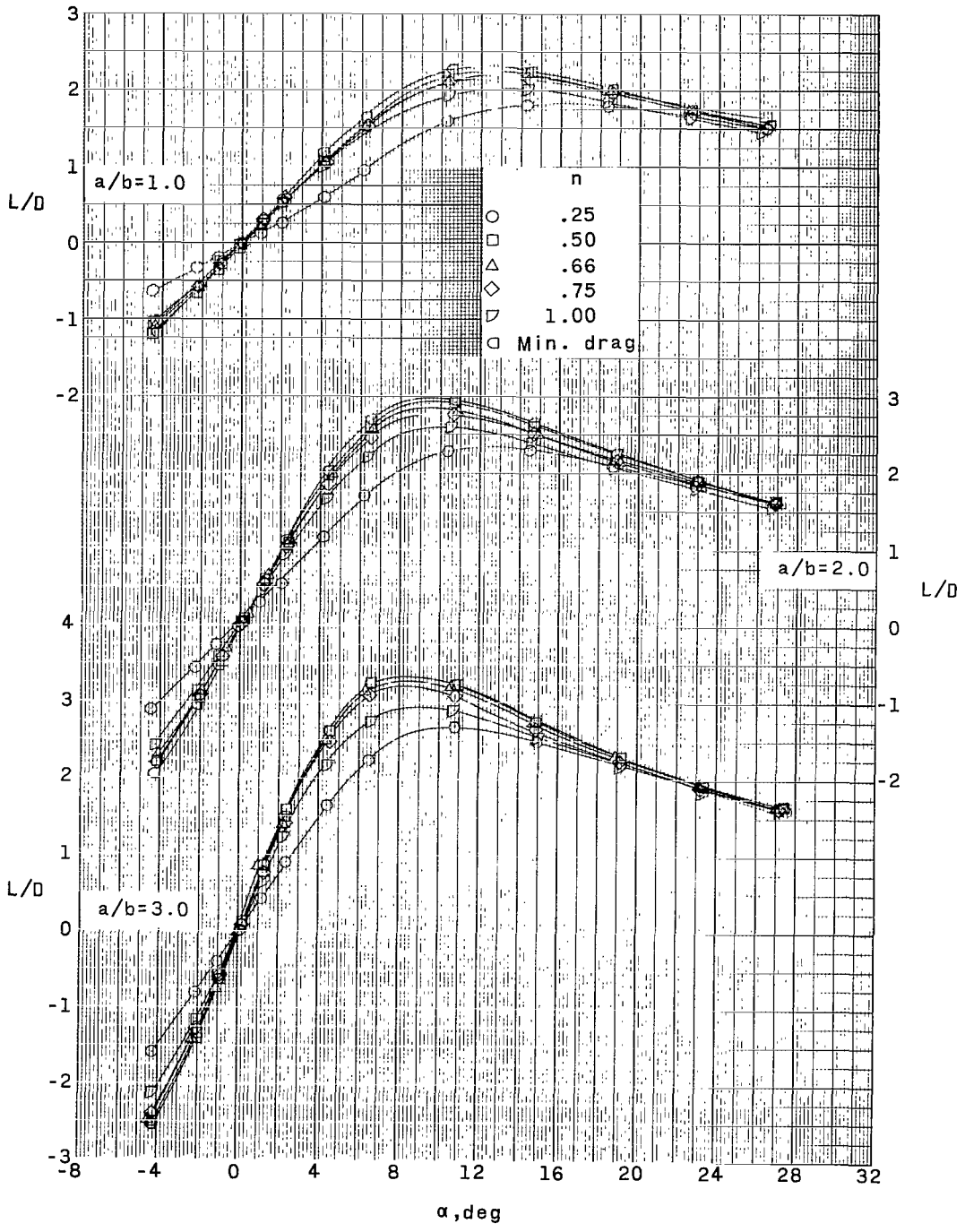

(c) L/D as a function of α.

Figure 9.- Continued.

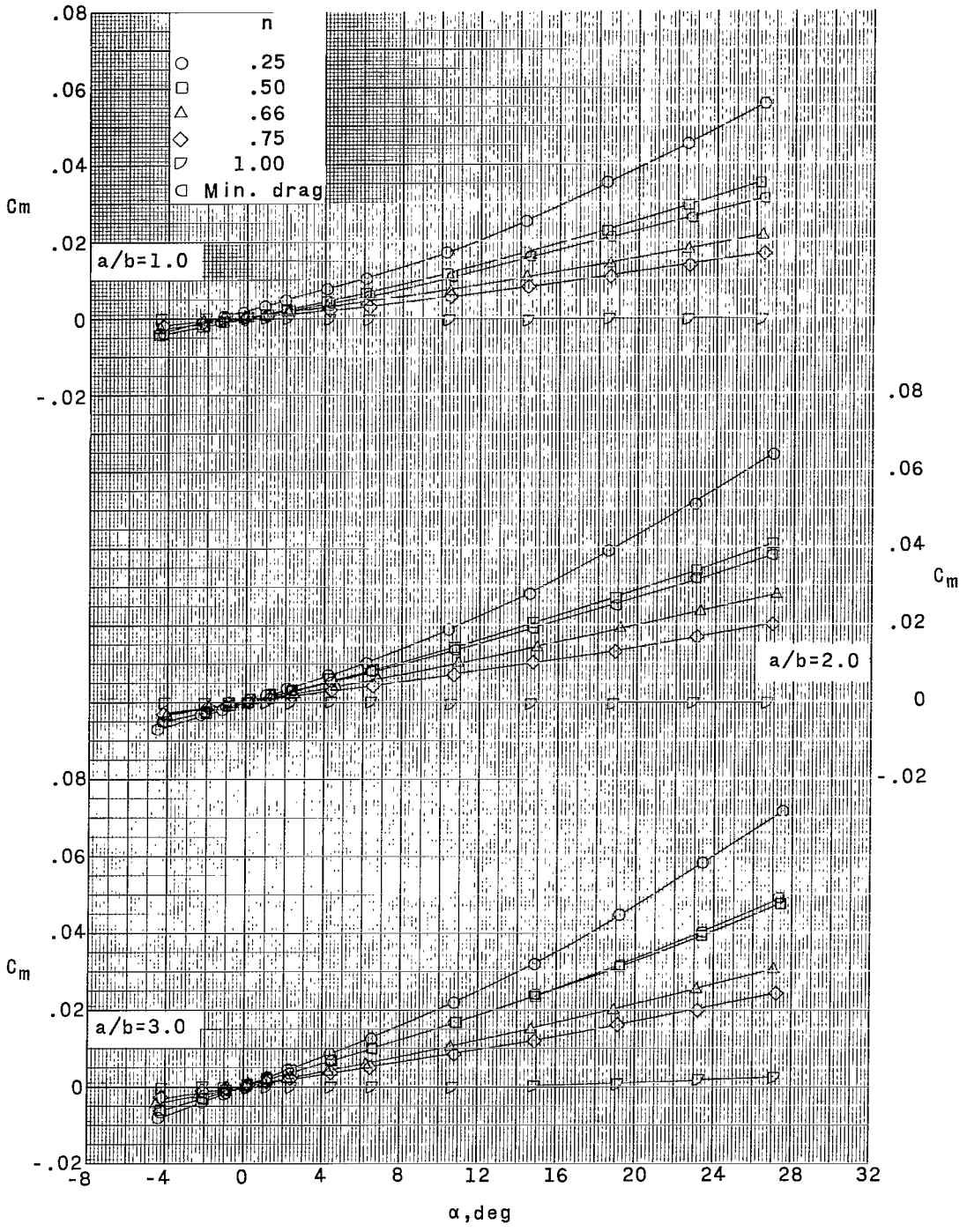

(d) C_m as a function of α.

Figure 9.- Concluded.

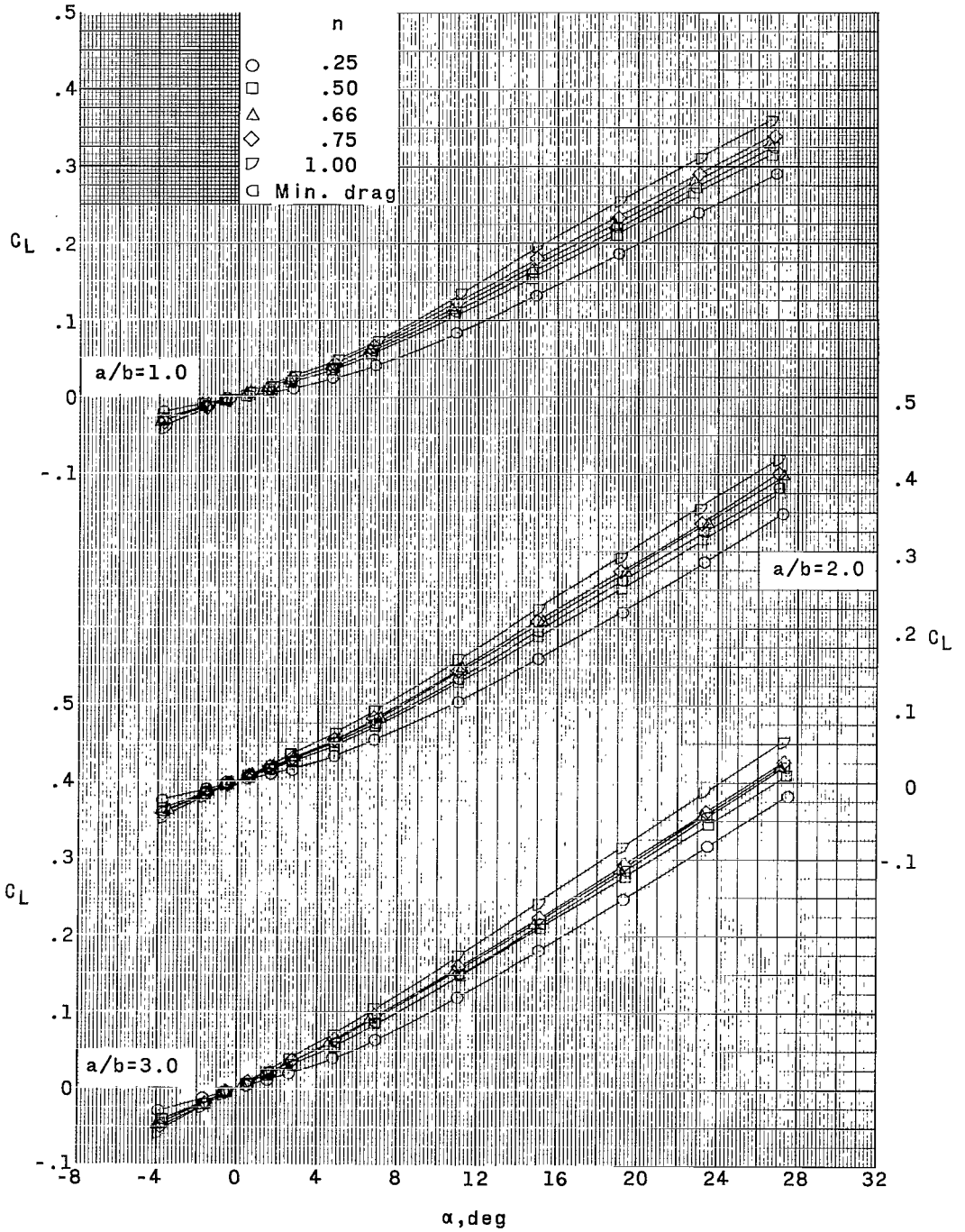

(a) C_L as a function of α.

Figure 10.- Longitudinal aerodynamic characteristics of power-law bodies and minimum-wave-drag body having variations in ellipticity at a Mach number of 4.63.

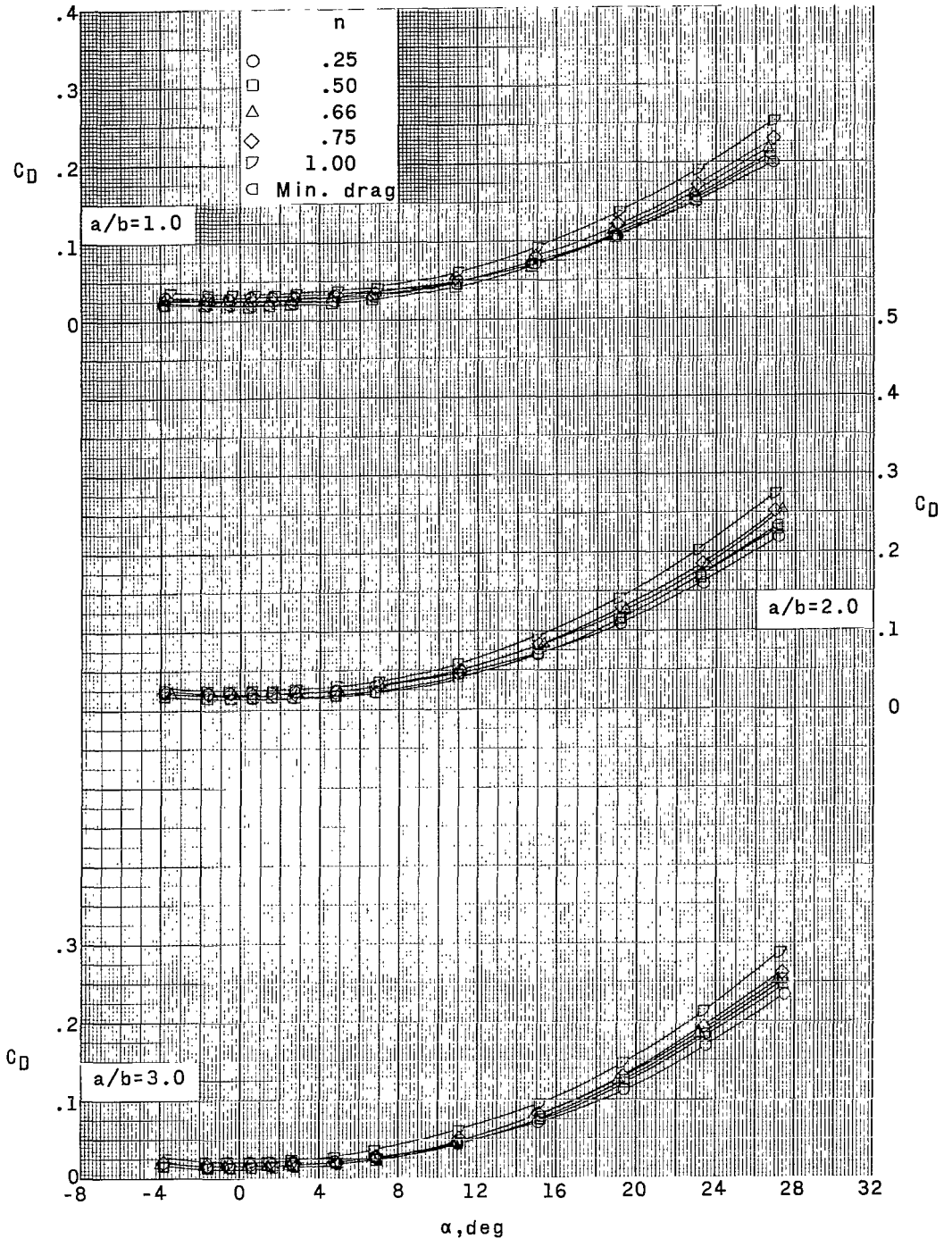

(b) C_D as a function of α.

Figure 10.- Continued.

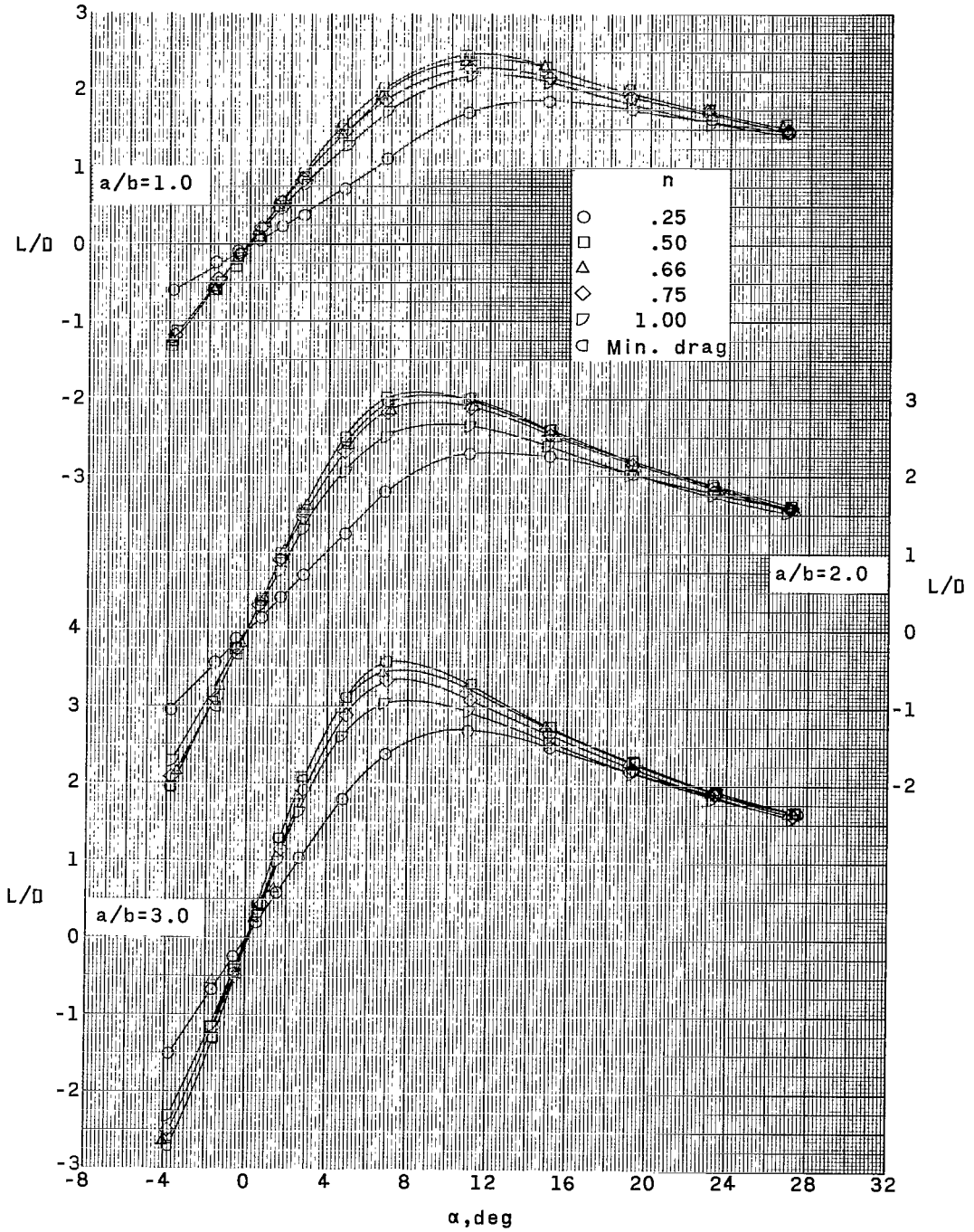

(c) L/D as a function of α.

Figure 10.- Continued.

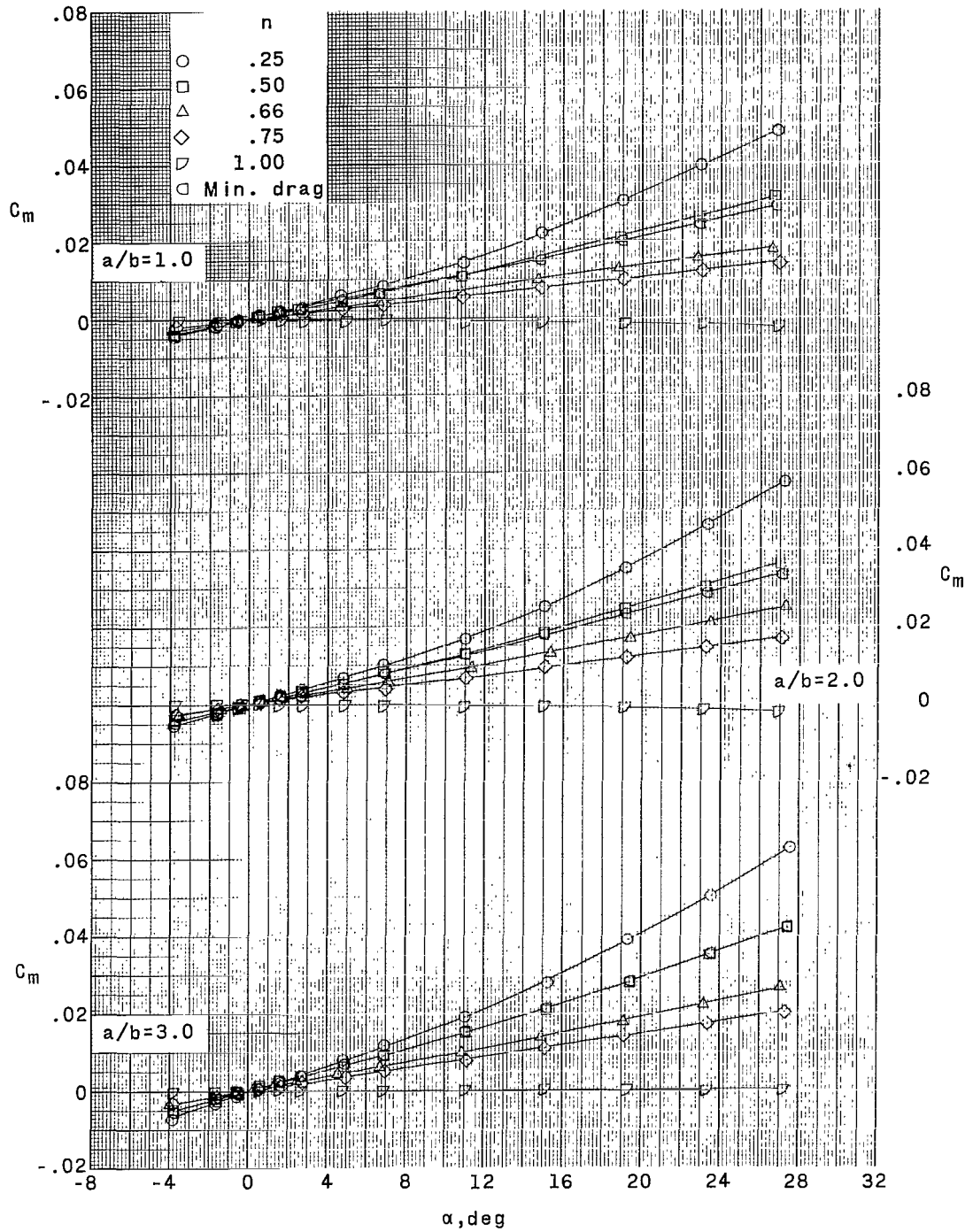

(d) C_m as a function of α.

Figure 10.- Concluded.

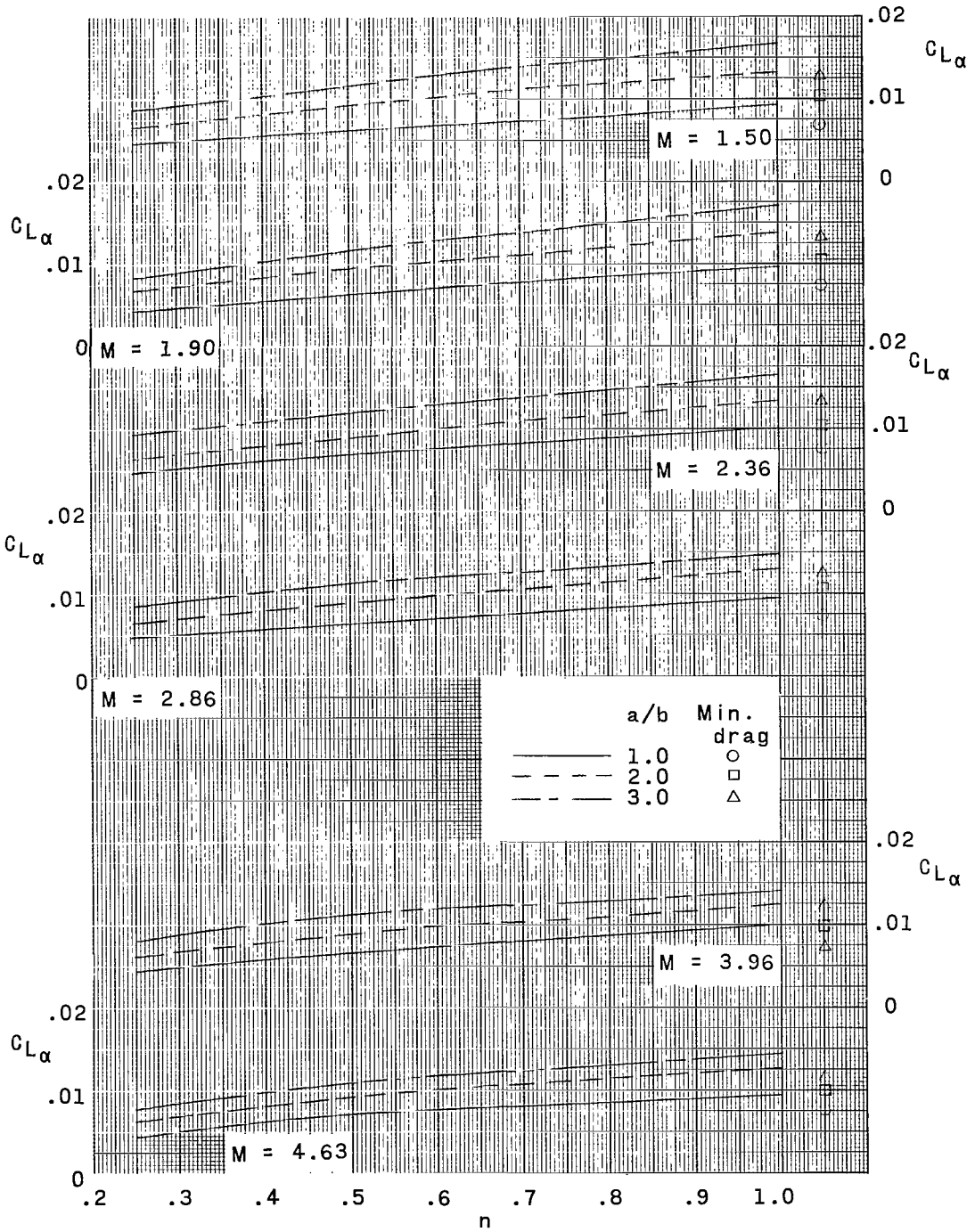

(a) C_{L_α} as a function of n.

Figure 11.- Variation of C_{L_α}.

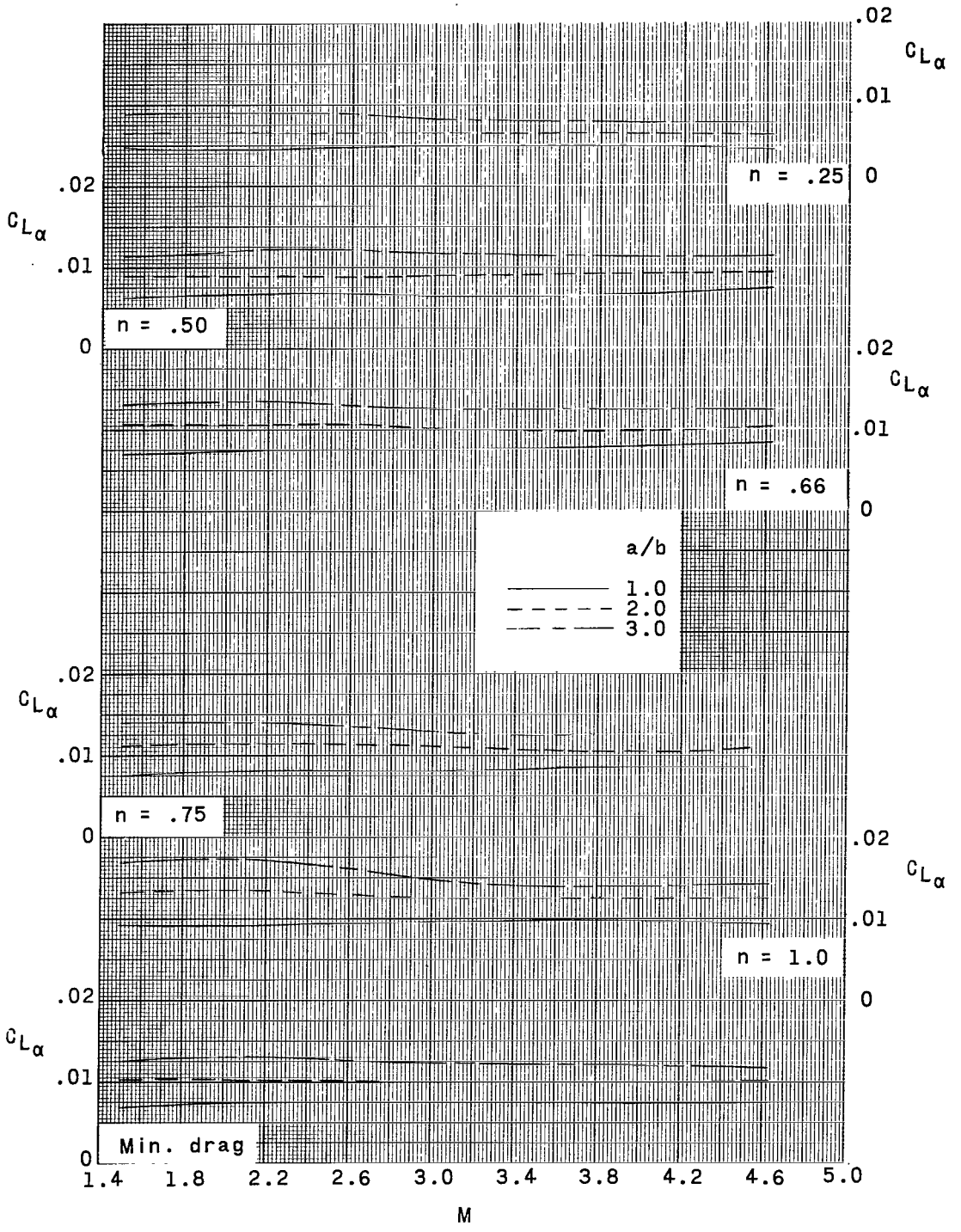

(b) C_{L_α} as a function of M.

Figure 11.- Concluded.

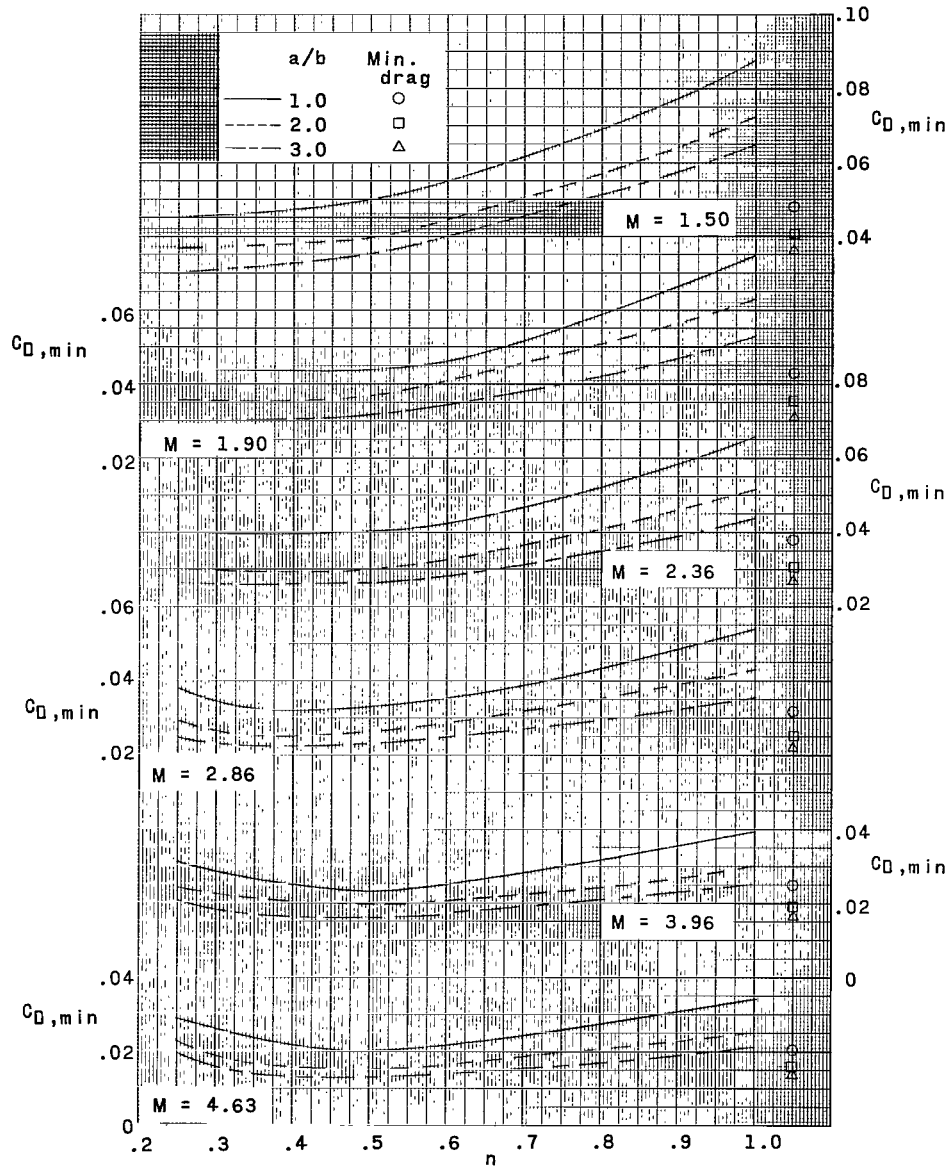

(a) $C_{D,min}$ as a function of n.

Figure 12.- Variation of $C_{D,min}$.

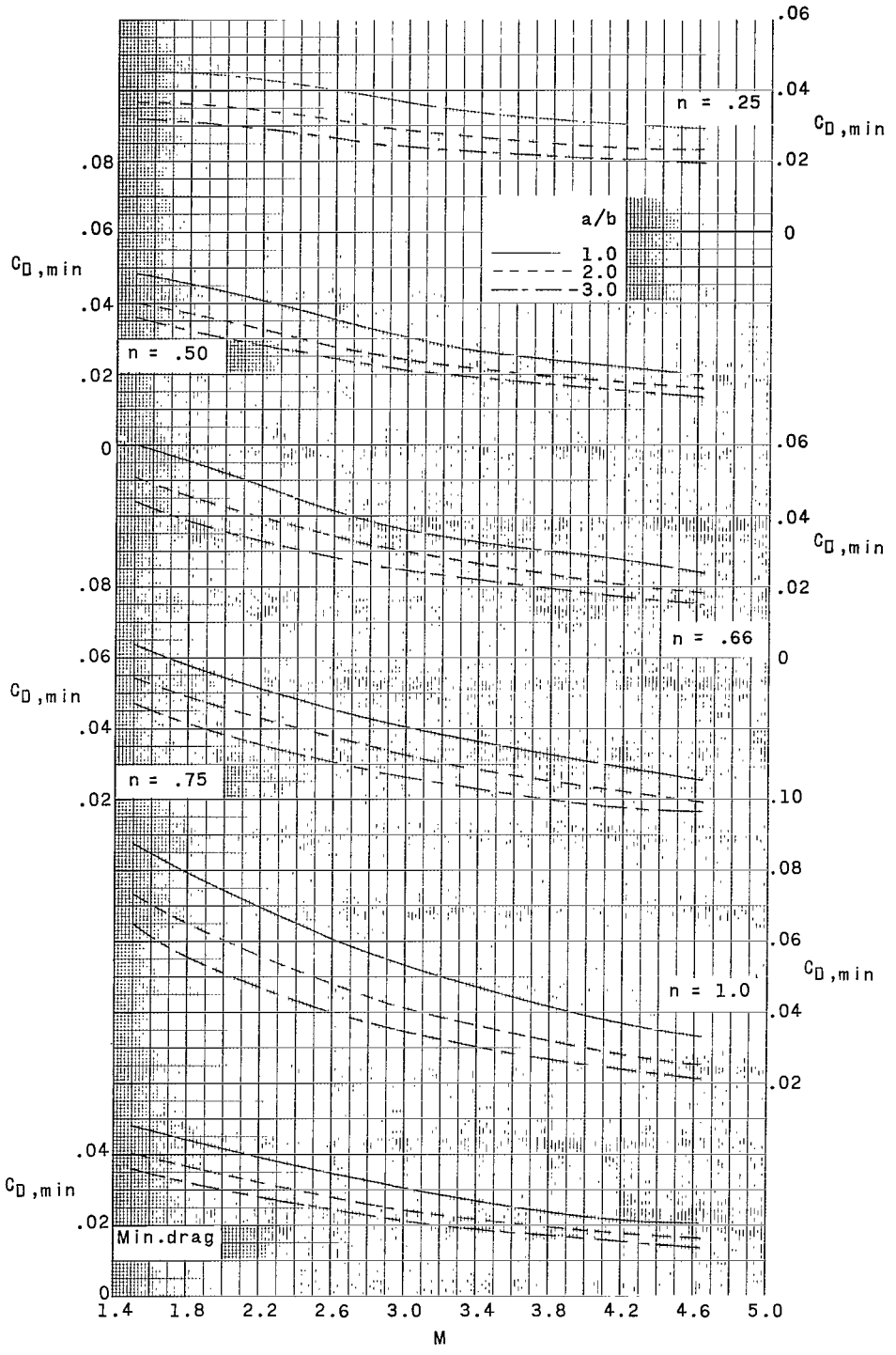

(b) $C_{D,min}$ as a function of M.

Figure 12.- Continued.

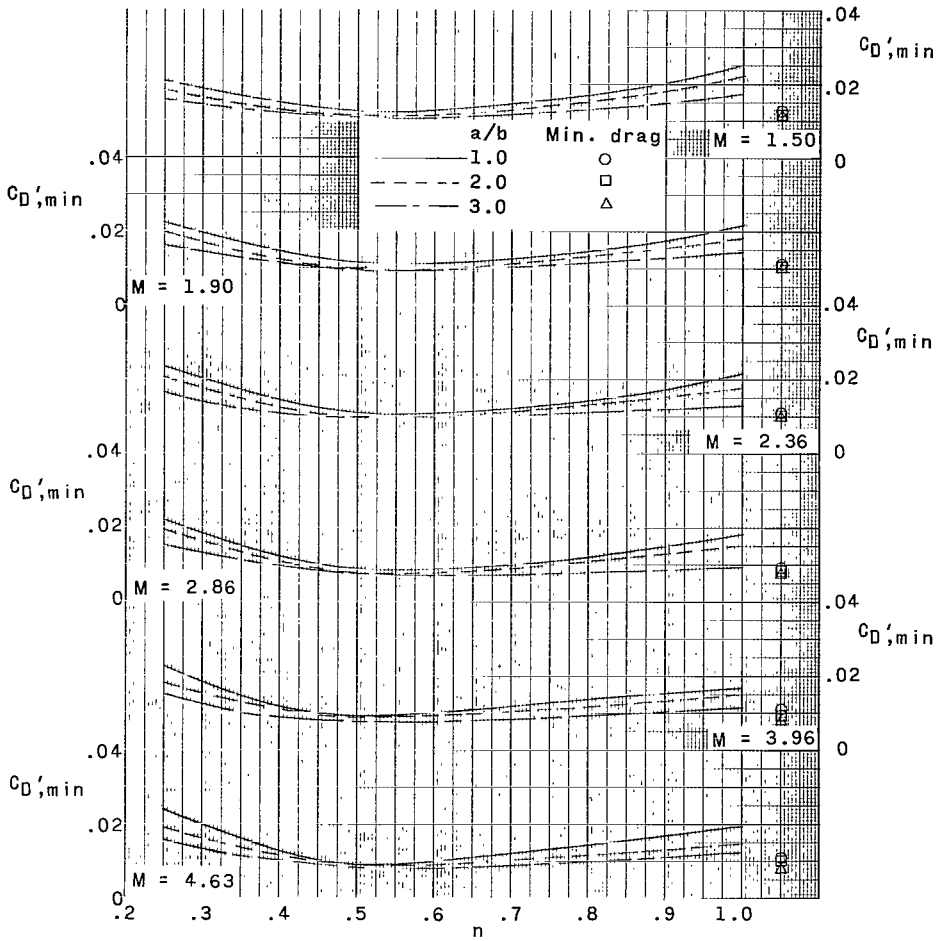

(c) $C'_{D,min}$ as a function of n.

Figure 12.- Continued.

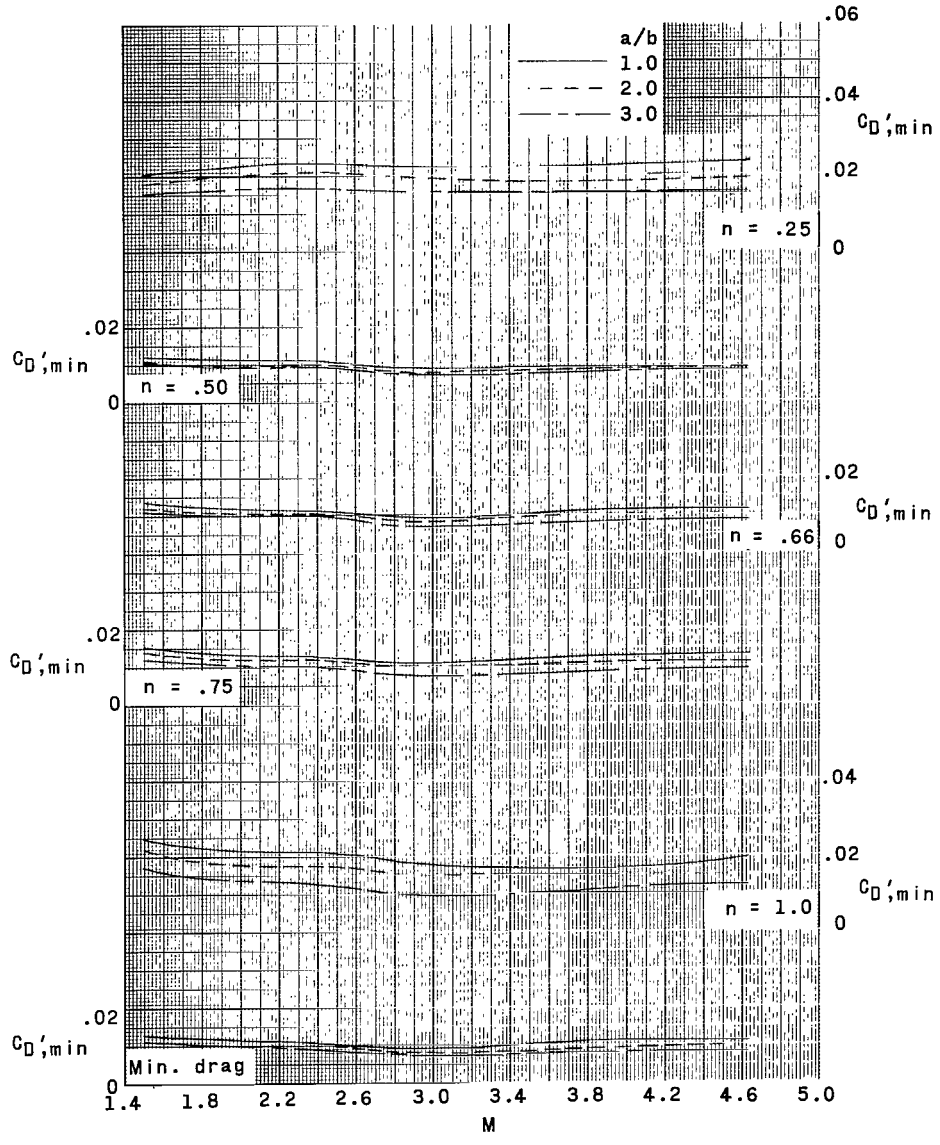

(d) $C'_{D,min}$ as a function of M.

Figure 12.- Concluded.

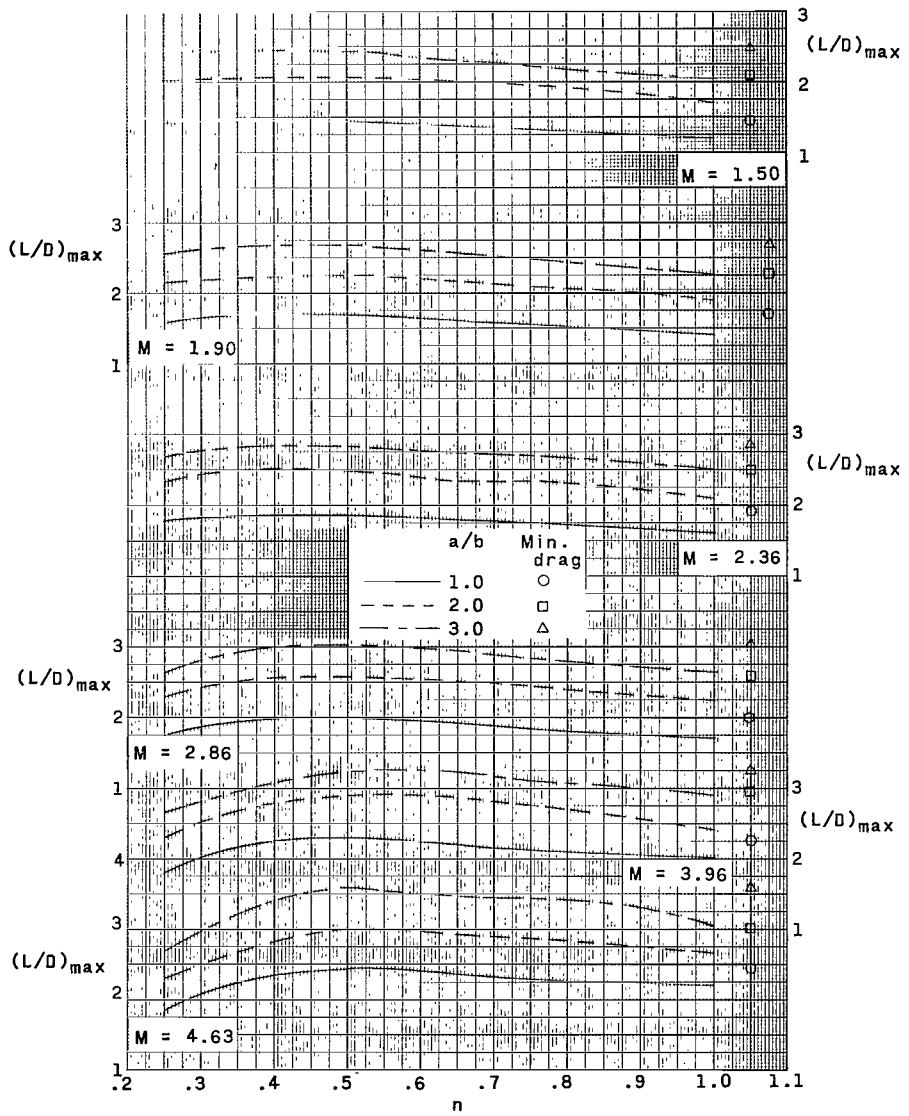

(a) $(L/D)_{max}$ as a function of n.

Figure 13.- Variation of $(L/D)_{max}$.

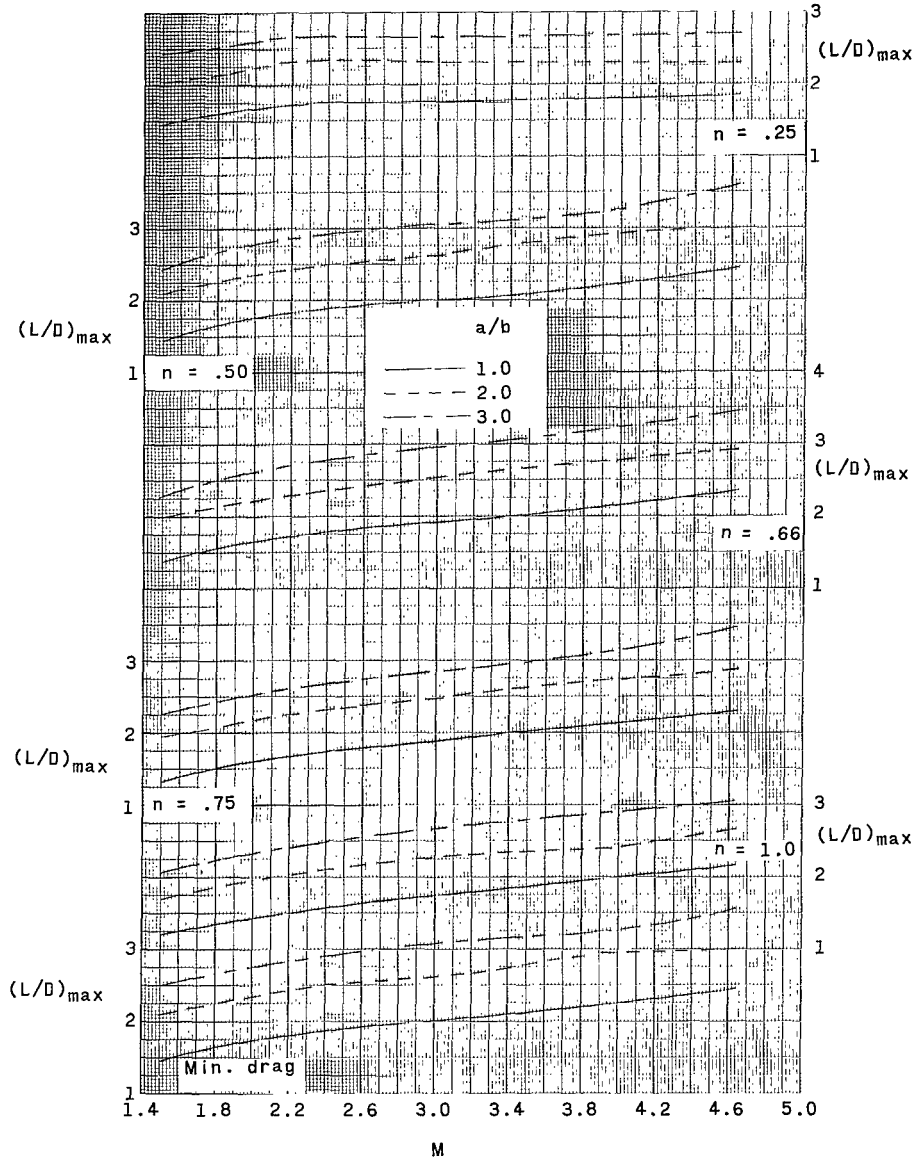

(b) $(L/D)_{max}$ as a function of M.

Figure 13.- Continued.

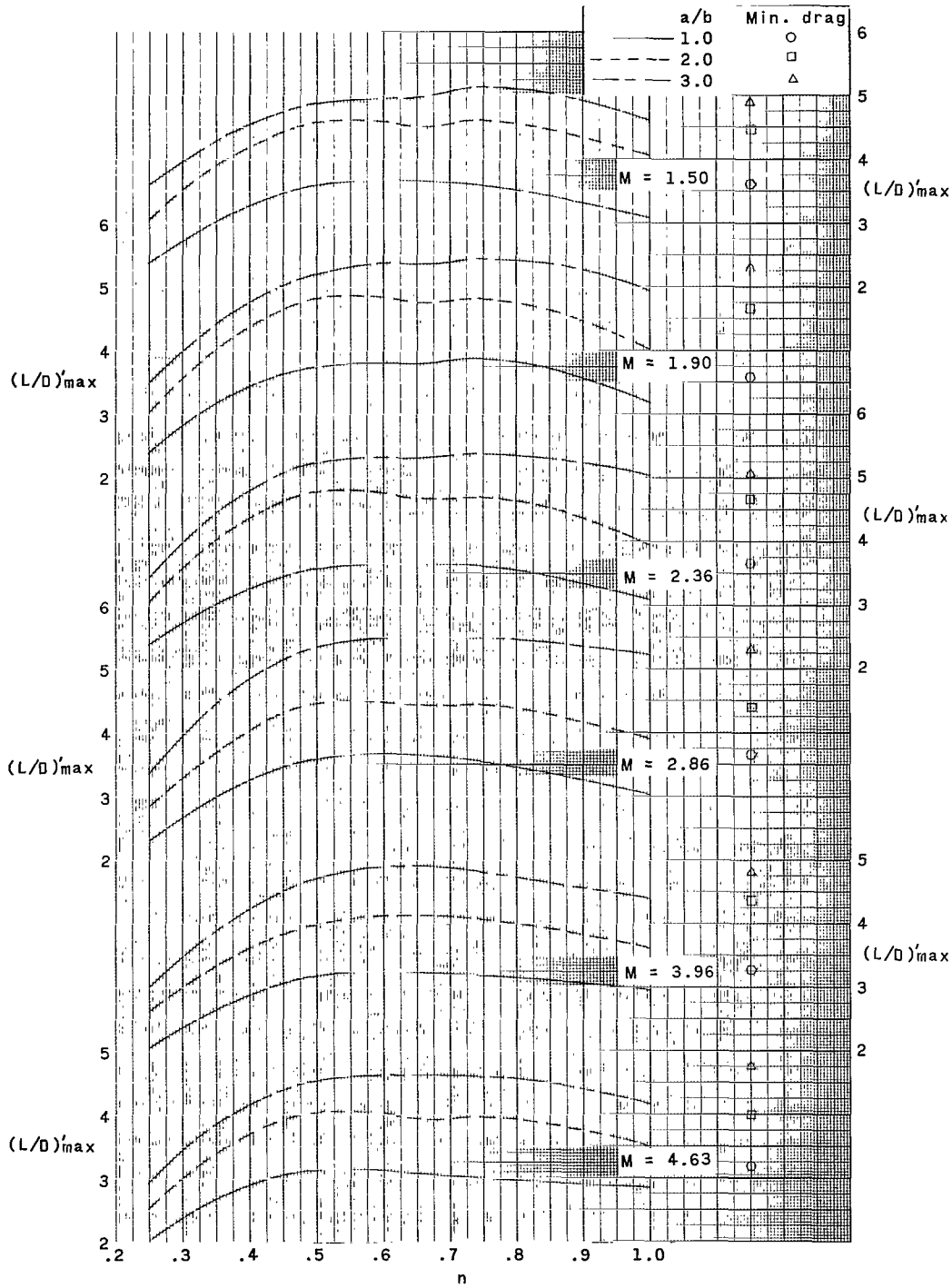

(c) $(L/D)'_{max}$ as a function of n.

Figure 13.- Continued.

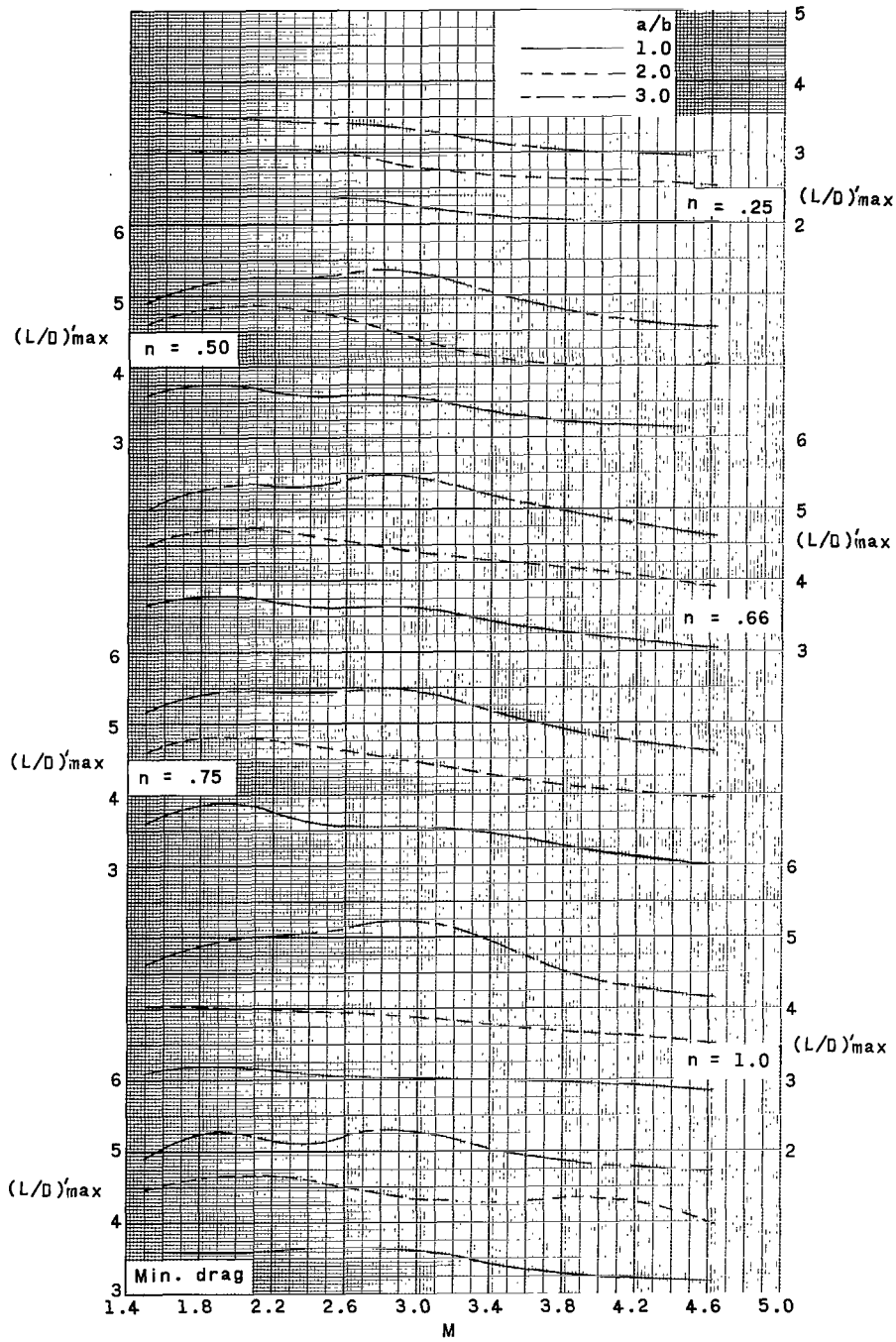

(d) $(L/D)'_{max}$ as a function of M.

Figure 13.- Concluded.

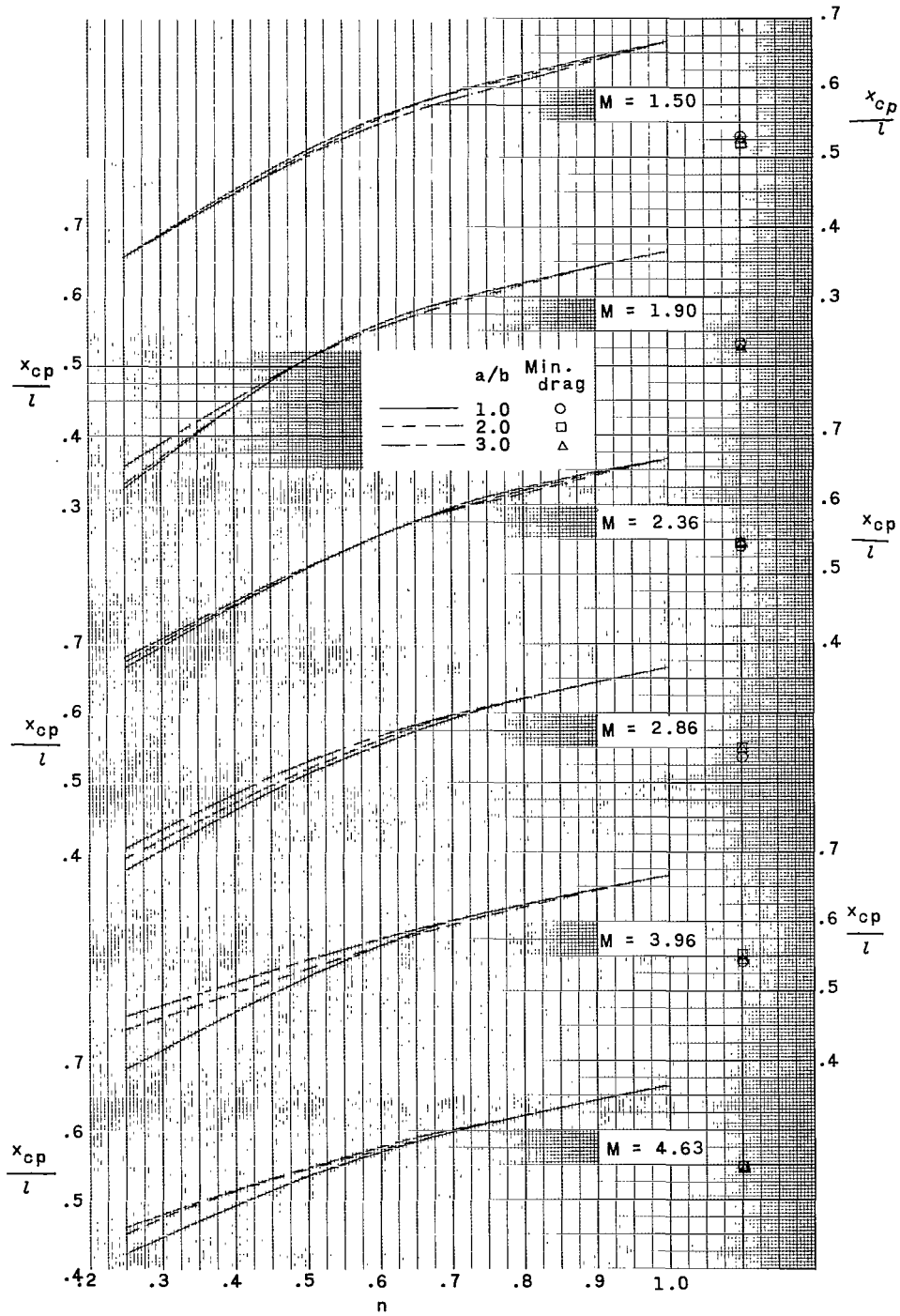

(a) x_{cp}/l as a function of n.

Figure 14.- Variation of x_{cp}/l.

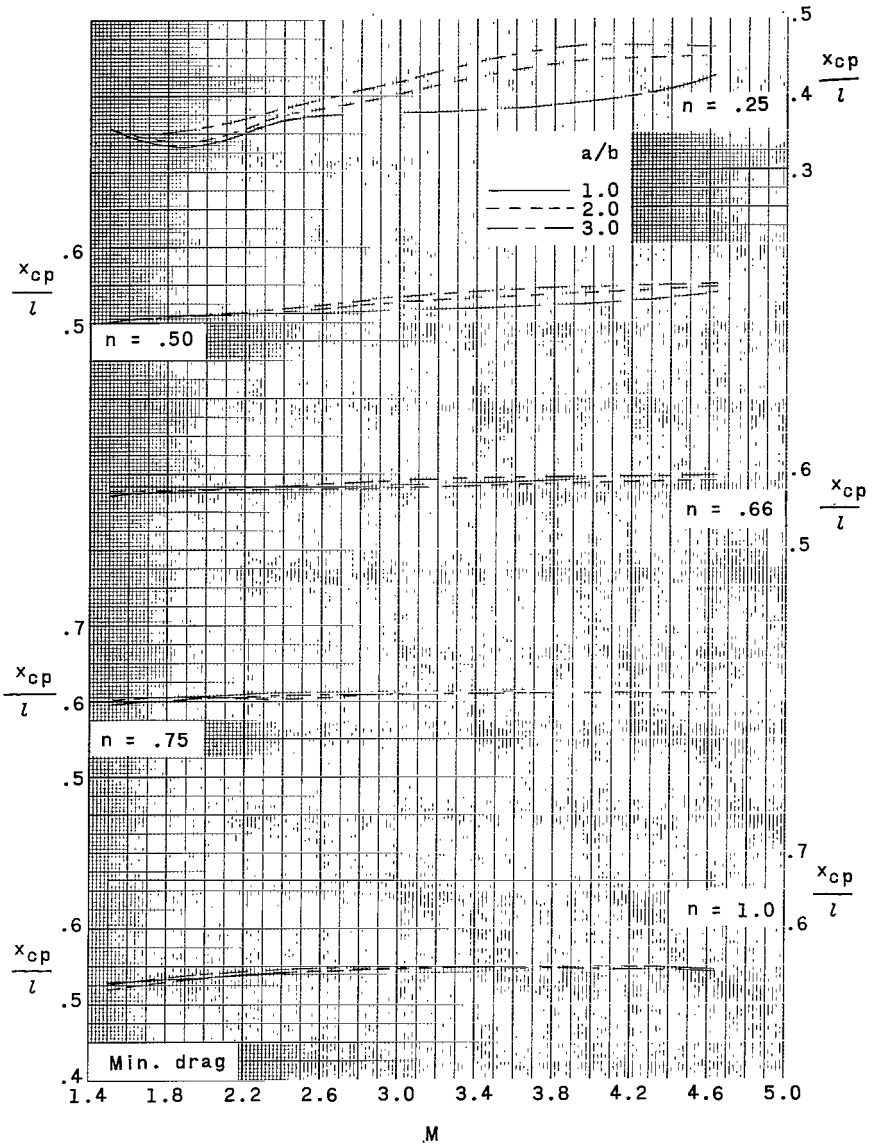

(b) x_{cp}/l as a function of M.

Figure 14.- Concluded.

"The aeronautical and space activities of the United States shall be conducted so as to contribute . . . to the expansion of human knowledge of phenomena in the atmosphere and space. The Administration shall provide for the widest practicable and appropriate dissemination of information concerning its activities and the results thereof."

—NATIONAL AERONAUTICS AND SPACE ACT OF 1958

NASA SCIENTIFIC AND TECHNICAL PUBLICATIONS

TECHNICAL REPORTS: Scientific and technical information considered important, complete, and a lasting contribution to existing knowledge.

TECHNICAL NOTES: Information less broad in scope but nevertheless of importance as a contribution to existing knowledge.

TECHNICAL MEMORANDUMS: Information receiving limited distribution because of preliminary data, security classification, or other reasons.

CONTRACTOR REPORTS: Technical information generated in connection with a NASA contract or grant and released under NASA auspices.

TECHNICAL TRANSLATIONS: Information published in a foreign language considered to merit NASA distribution in English.

TECHNICAL REPRINTS: Information derived from NASA activities and initially published in the form of journal articles.

SPECIAL PUBLICATIONS: Information derived from or of value to NASA activities but not necessarily reporting the results of individual NASA-programmed scientific efforts. Publications include conference proceedings, monographs, data compilations, handbooks, sourcebooks, and special bibliographies.

Details on the availability of these publications may be obtained from:

SCIENTIFIC AND TECHNICAL INFORMATION DIVISION

NATIONAL AERONAUTICS AND SPACE ADMINISTRATION

Washington, D.C. 20546